ORNL-2890
UC-81 Reactors – Power
TID-4500 (15th ed.)

MOLTEN-SALT REACTOR PROGRAM

QUARTERLY PROGRESS REPORT

FOR PERIOD ENDING OCTOBER 31, 1959

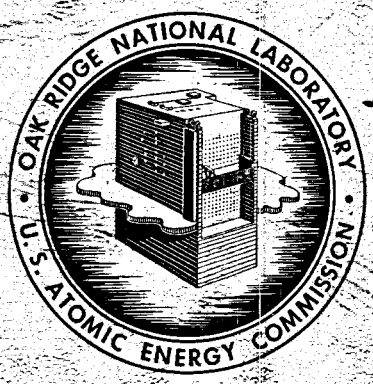

OAK RIDGE NATIONAL LABORATORY
operated by
UNION CARBIDE CORPORATION
for the
U.S. ATOMIC ENERGY COMMISSION

Printed in USA. Price $2.25. Available from the
Office of Technical Services
Department of Commerce
Washington 25, D.C.

ORNL-2890
Reactors – Power
TID-4500 (15th ed.)

Contract No. W-7405-eng-26

MOLTEN-SALT REACTOR PROGRAM

QUARTERLY PROGRESS REPORT

For Period Ending October 31, 1959

H. G. MacPherson, Project Coordinator

DATE ISSUED

MAR 8 1960

OAK RIDGE NATIONAL LABORATORY
Oak Ridge, Tennessee
operated by
UNION CARBIDE CORPORATION
for the
U.S. ATOMIC ENERGY COMMISSION

MOLTEN-SALT REACTOR PROGRAM QUARTERLY PROGRESS REPORT

SUMMARY

Part 1. Engineering and Component Development

1.1 Component Development and Testing

Development work on molten-salt-lubricated bearings was continued. In the series of seven concluded tests the start-stop tolerance of journal bearings made of INOR-8 was investigated. In all but two cases, tests were carried to seizure or impending seizure. Time of operation ranged from 3 to 379 hr. The largest number of start-stop cycles per test was 260. Signs of metal-to-metal rubbing were evident on bearing surfaces. Serious ingassing was observed during bench tests of the hydrodynamic thrust bearing. Remedial efforts are being continued, and further bench tests are proposed.

Two pumps equipped with hydrodynamic bearings were bench tested and then tested in molten salt. Seizure occurred in both after short operation in salt, and the failures were attributed to dry bearings caused by excessive restrictions in the suction path of the bearings.

No evidence of self-welding was found between INOR-8 surfaces immersed in molten salt at 1200°F. Coefficients of dry friction for INOR-8 on INOR-8 and for INOR-8 on stainless steel were found to be fairly constant in the 900 to 1800°F temperature range, a good average value being 0.25.

Construction of the Remote Maintenance Demonstration Facility, including the viewing equipment, was completed. The layout is being modified and additional maintenance tools are being made as need arises. The loop was tested for vacuum-tightness. The remote viewing equipment was modified to improve its reliability and picture quality. A set of four television cameras provides nearly 90% viewing coverage of the cell. All major components except the core vessel have been disconnected and reinstalled by remote means at least once. The loop will be run with molten salt after removal and installation of the core vessel have been successfully accomplished.

Eleven long-term corrosion loops completed one year of operating time in this quarter. Tests on two INOR-8 loops and one Inconel loop were terminated for metallurgical examination; the results are not yet available.

One loop was shut down temporarily due to pump failure and a subsequent oil fire. The test will be continued after repairs and reloading. The second of three sample inserts was removed from loop 9354-4 after 10,000 hr of operation. Findings on this insert are described in Sec 2.1. Two new INOR-8 loops were started up with BULT-14 salt. These loops have double-walled inserts at the exit of the second resistance heater.

The PKP centrifugal pump with Fulton Sylphon bellows-mounted seal has logged 17,878 hr of operation in NaK at 1200°F. Only negligible leakage was observed. The MF-type centrifugal pump is operating in a region of cavitation in salt 30, and service time of more than 20,000 hr has been recorded to date. The average upper- and lower-seal leakage rates amounted to 30 and 12 cc/day, respectively.

Trouble-free operation of the small frozen-lead pump seal continued. Total service time is 12,000 hr. The large frozen-lead-seal test was discontinued.

An apparatus for testing graphite-metal seals is under construction. A seal in the annulus between a 5-in.-OD graphite tube and a larger, mating Inconel section will be attempted first.

Sectioning of the first two in-pile loops was completed, and metallographic and analytical examinations are in progress. A test program was launched to explore the behavior of graphite under conditions similar to those encountered in graphite-moderated molten-salt reactors. Bench tests have been completed, and the first experiment is scheduled for insertion in the MTR early in 1960.

1.2 Engineering Research

The viscosity of the fuel mixture BULT-14 (LiF-BeF_2-UF_4-ThF_4, 67-18.5-0.5-14 mole %) was determined in the temperature range from 550 to 800°C. Comparison with previous results on other salt compositions containing a high percentage of ThF_4 shows a maximum deviation of 18% at the extremes of the temperature range. Enthalpy measurements with the BeLT-15 mixture (LiF-BeF_2-ThF_4, 67-18-15 mole %) yielded a heat capacity varying from 0.343 $Btu \cdot lb^{-1} \cdot (°F)^{-1}$ at 1000°F to 0.304 $Btu \cdot lb^{-1} \cdot (°F)^{-1}$ at 1500°F. The apparatus for measuring the thermal expansion coefficient, β, of molten salt mixtures was tested by using HTS ($NaNO_2$-$NaNO_3$-KNO_3, 40-7-53 wt %). The coefficient β was 3.63×10^{-4}/°C between 215 and 315°C; comparison with data obtained from density measurements shows good agreement.

Preliminary results were obtained for heat transfer with BULT-14 flowing in heated Inconel and INOR-8 tubes. The system was operated continuously for about five weeks without difficulty. Axial temperature profiles show the effect of the laminar-turbulent transition in the hydrodynamic boundary layer in the entrance section of the tube. The heat transfer appears to be about half that which would be predicted from earlier studies with molten salts; this discrepancy may result from an uncertainty in the value of the thermal conductivity for BULT-14 used in the analysis of the data. A 23% difference between the results in the Inconel and INOR-8 tubes cannot be explained, at present.

Part 2. Materials Studies

2.1 Metallurgy

In an effort to join graphite to graphite and graphite to metal for molten-salt reactor service, an alloy (48% Ti–48% Zr–4% Be) was developed and had satisfactory wetting and flowing characteristics. However, because of its poor corrosion resistance to molten fluorides, other alloy systems are being investigated. Promising alloys in the Au-Ni-Ta system are under study, and alloys in the Ni-Nb, Ni-Mo, Ni-Nb-Mo, Ni-Nb-Ta, Pd-Ni-Ta, and Pd-Ni-Mo systems are being prepared for testing. Preliminary work in electric-resistance brazing of graphite to graphite, using molybdenum as the brazing alloy, has also been undertaken.

The second of three INOR-8 corrosion inserts was removed after 10,000 hr from an INOR-8 forced-convection loop. Weight-loss evaluations indicated the insert to have lost 2.0 mg/cm^2, which corresponds to a wall thickness decrease of 0.09 mil, if uniform removal of the wall is assumed. Examination of three Inconel forced-convection loops, which circulated fluorides for one year, was completed. Two of the loops showed normal attack in the form of intergranular and general voids to a depth ranging from 1 to 14 mils. The third loop was heavily attacked to depths ranging from 18 to 38 mils. Salt in the latter loop showed appreciable oxide contamination.

Fifteen grades of graphite were classified according to their resistance to permeation by molten fluorides at 150 psig at 1300°F in 100-hr tests. Grade GT-123 was found to have a bulk-volume permeation of less than 0.5%, the maximum specified for the reactor, despite the high test

pressure. Bismuth has been used to fill the accessible voids in AGOT graphite prior to exposing it to molten salts. Tests are being conducted to determine to what extent the bismuth-permeated graphite will pick up salts during standard permeation tests.

When held in direct contact with graphite for 20 hr at 1300°F, LiF-BeF_2-UF_4 (62-37-1 mole %) apparently gettered completely the oxide contaminants in the graphite. No precipitation was detected radiographically in the LiF-BeF_2-ThF_4-UF_4 (67-18.5-14-0.5 mole %) after it had been in contact with graphite for 500 hr at 1300°F in a vacuum.

INOR-8 specimens showed no metallographic indications that carburization had occurred after being in contact with TSF graphite at 1000 psi for 700 hr in salt environment at 1300°F.

Four braze materials showed good resistance to fuel 130 (LiF-BeF_2-UF_4, 62-37-1 mole %) during a 5000-hr corrosion test in a thermal-convection loop with a 1300°F hot-leg temperature. Corrosion tests of 100-hr duration indicated that the usefulness of titanium-, zirconium-, or beryllium-containing brazing alloys in fuel 130 would be limited in pure nickel or INOR-8 containers at 1300°F. Heavy attack due to the transfer of the refractory material to the nickel or INOR-8 container walls was observed.

2.2 Chemistry and Radiation Effects

Detailed description of the ten subsidiary binary and ternary systems incorporated in the LiF-BeF_2-UF_4-ThF_4 quaternary system is nearly completed. Among the questions as yet incompletely answered by phase-equilibria studies on breeder fuels is that of detailed crystallization paths for compositions of reactor interest.

The identification of the isomorphic compounds $NaF \cdot BeF_2 \cdot 3UF_4$ and $NaF \cdot BeF_2 \cdot 3ThF_4$ is of especial academic interest since $NaF \cdot BeF_2 \cdot 3UF_4$ has been erroneously reported in the literature as $NaF \cdot 4UF_4$.

The solubility of HF in molten fluoride breeder fuels has been correlated with solvent composition by means of a concentration scale based on the excess or deficiency, in equivalent per cent, of alkali fluoride for complete coordination of higher-valence cations in the solvent; that is, Na_2BeF_4 and Na_3ZrF_7 correspond to complete coordination and represent the limit of complexing power of the cation.

Exchange reactions in molten fluorides, particularly those that might be of interest in reprocessing schemes, are being explored. Many of the

reactions potentially useful for removing rare earths are subject to interference by essential ingredients in the fuel.

The diffusion of chromium, which is the rate-limiting process for long-term corrosion in molten fluoride breeders, is strongly dependent on grain size, and hence on annealing history. Under equivalent conditions there is no significant difference between the diffusion coefficients of chromium in INOR-8 and in Inconel; thus the steady-state corrosion rate is predicted to be higher by a factor of 15/7 in Inconel, since this is the ratio of chromium concentration in the two alloys.

Except for one unexplained and palpably misfunctioning case, sampled corrosion test loops are demonstrating predictable and satisfactory behavior in long-term tests.

Exploratory studies on the hygroscopicity of fuels and on the possibility of drying at low temperatures without extensive hydrolysis have given additional qualitative evidence of the extreme sensitivity of the fuels to moist air.

Evidence of formation of a graphite intercalation compound with MoF_5 was found, but this compound is not expected to be encountered in reactor operation.

Several grades of extruded graphite, but none of the molded types, show less than 1 vol % permeation by breeder fuels at 60 to 75 psig and 1300°F.

About 740 kg of purified fuel mixtures was processed during the quarter. INOR-8 corrosion test capsules have been removed from the MTR after 5500 hr of exposure and a 75% uranium burnup.

2.3 Fuel Processing

Modification of the hydrofluorination–volatilization process is being investigated for application to thorium-bearing fuel salts, a principal objective being the retention of the processed material in the fluoride form. The solubility of ThF_4 in hot aqueous ammonium fluoride solutions is as high as 4 to 5%, and this system is therefore being investigated further. The use of ClF_3-HF mixtures does not appear feasible because of the suppression of LiF solubility and the correspondingly low UF_4 and ThF_4 solubilities. The NO_2-HF system is also unattractive because of the low solubility of ThF_4, although that of UF_4 is higher.

CONTENTS

PART 1.

ENGINEERING AND COMPONENT DEVELOPMENT

1.1 COMPONENT DEVELOPMENT AND TESTING

Molten-Salt-Lubricated Bearings for Fuel Pumps

Hydrodynamic Journal Bearings

Investigations of journal bearings operating in molten salt 130 (LiF-BeF_2-UF_4, 62-37-1 mole %) were continued throughout the quarter. Four tests were performed to investigate start-stop ability of carburized INOR-8 journals operating at temperatures from 1200 to 1500°F in INOR-8 bearings having three axial grooves; three were conducted to investigate performance of the three-helical-groove INOR-8 bearing at 1200°F. A test, No. 22, of the performance of Inconel for comparison with INOR-8 is in progress. All test pieces were fitted with a radial clearance of 0.005 in. (measured at room temperature). A summary of the test conditions is presented in Table 1.1.1.

Test 15 was terminated when impending seizure became evident upon restarting the run following a 30-min shutdown for repairs in the off-gas line. The support pins were twisted and partially severed from the bearing sleeve. This condition, a result of poor attachment, possibly gave rise to the impending failure.

Test 16, which was a repeat of test 15 with new parts, was terminated on schedule. Examination indicated that rubbing damage was somewhat less than that experienced during a similar test at 1200°F.

Test 17 was terminated by seizure during start-stop cycle 129. The test pieces exhibited galling and metal transfer, evidences of rubbing.

Test 18 was conducted until seizure occurred between the bearing and journal. They did not meet dimensional specifications; the test should therefore be repeated.

Test 19 was conducted with bearing grooves having a cross-sectional area less than that used in the other tests with helical-groove bearings. Flow passage was not restricted at the discharge end of the grooves. Seizure was impending when an attempt was made to place the bearing back in operation after the test had been stopped for a start-stop operation following a test at 300 lb_f. Signs of rubbing were evident on the test pieces.

Test 20 was performed with bearing grooves of the same cross section as that used in test 19, but with a flow restrictor over the discharge

Table 1.1.1. Hydrodynamic-Journal-Bearing Tests; Summary of Test Conditions

Test No.	Material		Groove Configuration*	Speed (rpm)	Operating Temperature (°F)	Radial Load (lb_f)	Operating Time (hr)	Start-Stop Cycles
	Bearing	Journal						
15	INOR-8	INOR-8, carburized	Axial	1200	1200 1300	200	21 24	2
16	INOR-8	INOR-8, carburized	Axial	1200	1300	200	123	260
17	INOR-8	INOR-8, carburized	Axial	1200	1400	200	94	129
18	INOR-8	INOR-8, carburized	Axial	1200	1500	200	3	1
19	INOR-8	INOR-8	Helical	1200	1200	10–300	136	1
20	INOR-8	INOR-8	Helical	1200	1200	10–150	22	1
21	INOR-8	INOR-8	Helical	1200 600	1200 1200	500 375	379	106
22	Inconel	Inconel	Axial	1200	1200	200	336	10

*All bearings contained three grooves.

end of the grooves. The flow restrictor was a thin disk having an inside diameter 0.010 in. larger than the inside diameter of the bearing. The test was terminated because of a slight roughness in the drive-motor power trace. Examination of the test pieces did not reveal any apparent cause for this problem.

Test 21 was a continuation of test 20, except that the flow restriction on the bearing grooves was reduced by adding a 1/16- by 1/16-in. V-notch to the shim at each groove. The test was terminated by apparent seizure in the 600-rpm run with 375 lb_f load. There was slight evidence of rubbing between the test surfaces.

Test 22, now in progress, is being performed with an Inconel journal and a three-axial-groove Inconel bearing.

Hydrodynamic Thrust Bearings

Bench tests were performed on the thrust-bearing tester with the thrust bearing immersed in oil. Gross ingassing was found, and a number of modifications were investigated as possible corrective measures. Several of these were promising, but further bench testing with other modifications is in order prior to hot tests in molten salt.

Test of Pump Equipped with One Molten-Salt-Lubricated Journal Bearing

Bench tests were conducted on the original pump design, shown in Fig. 1.1.1, to investigate the performance of the overhung motor, of the oil slinger in pumping lubricant to the upper bearing, and of the journal bearing immersed in oil.

The overhung motor was found to exert a large rotating radial load. Investigations show, however, that the load can be reduced to tolerable levels if the electrical balance of the motor is improved. In the interest of speeding the investigation of a molten-salt bearing applied to a pump, the overhung motor was temporarily replaced by a conventional motor with a flexible shaft coupling (Fig. 1.1.2), which will isolate the pump shaft from the effects of imbalance in the motor.

The oil slinger had to be modified before satisfactory flow of lubricant to the upper bearing could be attained. The modifications consisted of slitting the slinger and increasing the diameter of the oil return ports.

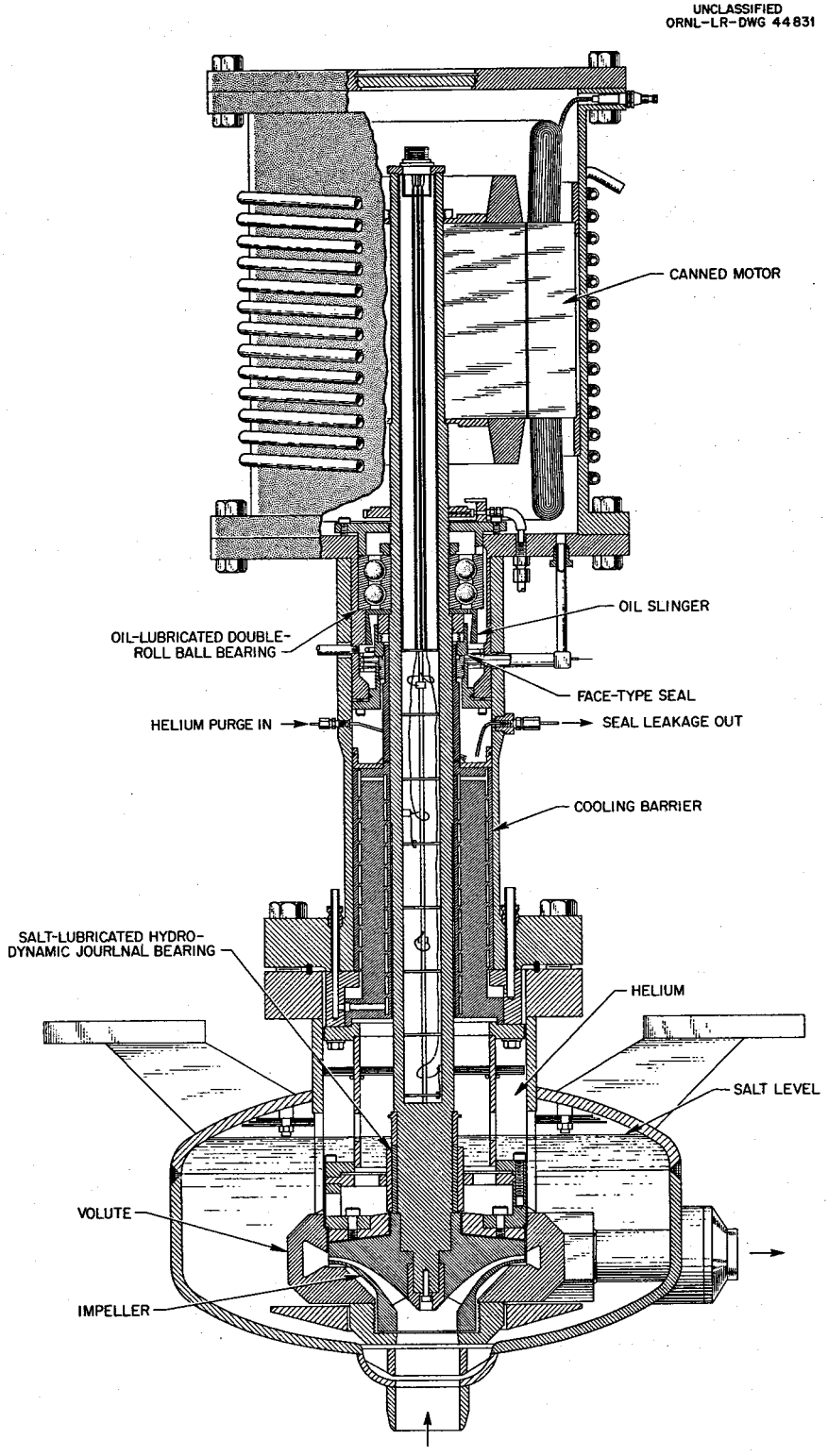

Fig. 1.1.1. Pump with Molten-Salt-Lubricated Journal Bearing and with an Overhung Motor.

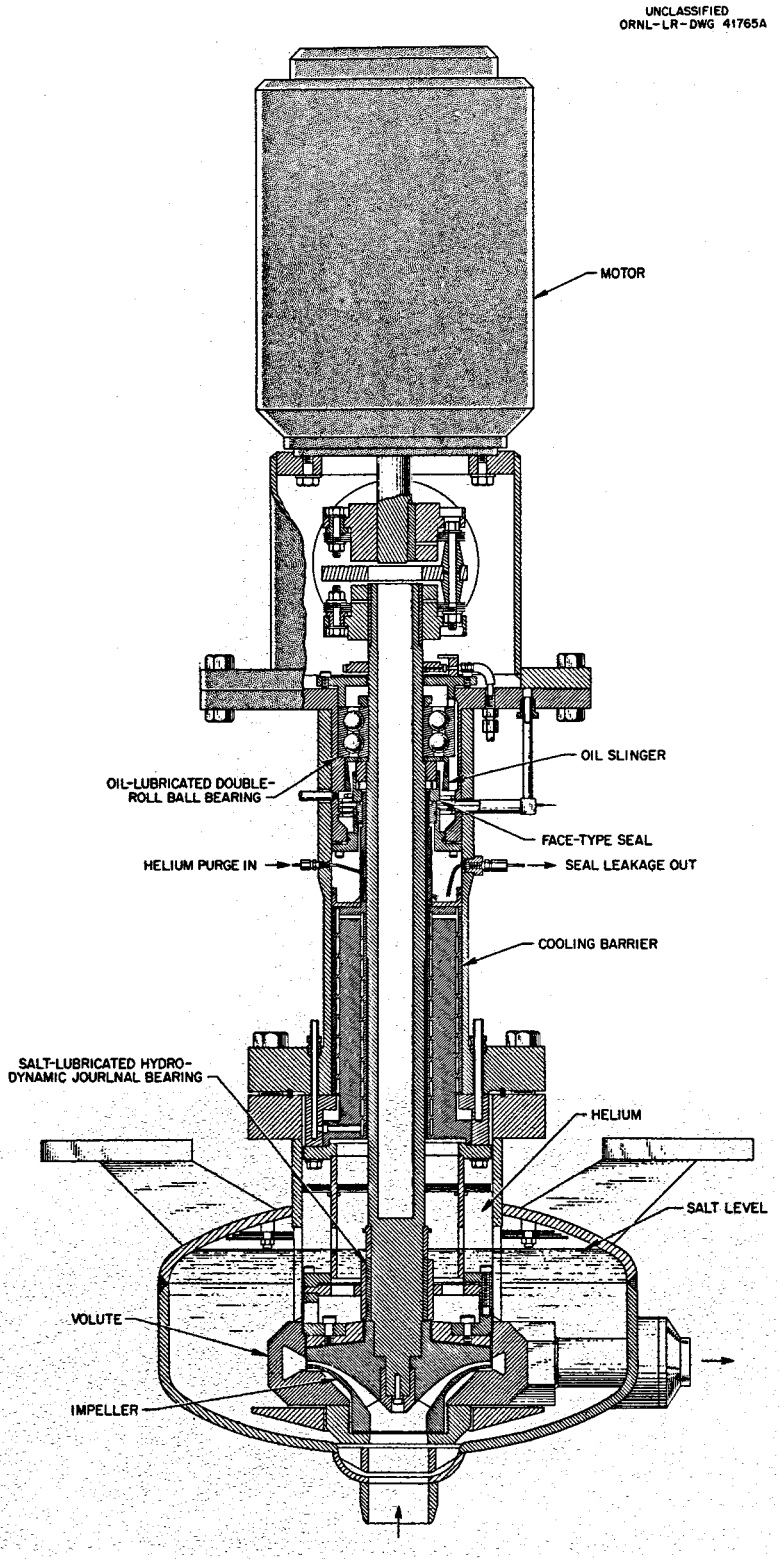

Fig. 1.1.2. Pump with Molten-Salt-Lubricated Journal Bearing and with a Flexible Shaft Coupling to a Conventional Motor.

Two journal-bearing configurations were tested in oil at room temperature and in molten salt 130 ($LiF-BeF_2-UF_4$, 62-37-1 mole %) at 1200°F. The oil tests were performed with the pump assembled except for the impeller; the complete assembly was operated in the tests with molten salt. The first bearing tested had three axial grooves and was mounted rigidly. The bearing operated successfully in oil under load, and the pump was subsequently placed in operation with molten salt. The pump was rotated for 10 min at 1000 rpm and another 10 min at 1200 rpm; at 1200 rpm the pump delivered a flow of 100 gpm. The operation was terminated as a result of seizure of the pump rotary element, which is believed to have occurred in the molten-salt-lubricated journal bearing.

The other bearing had three helical grooves with a flow restriction at the discharge (upper) end. The bearing was mounted flexibly on gimbals. It operated satisfactorily in oil but subsequently failed by seizure in operation with molten salt.

Study of the configuration near the bearing revealed that the impeller hub probably presented too great a restriction to flow of salt into the bearing at the lower end; the bearing therefore pumped itself dry in the molten-salt tests. This condition was probably responsible for both the failures. During the oil tests this condition was not present, since they were made without the impeller present. The flow passage into the bearing has been increased by removal of material from the impeller hub and the lower end of the bearing sleeve. Preparations are being made for a third test.

Self-Welding of INOR-8

One INOR-8 self-welding experiment was performed at 1200°F, on loose-fitting pins pressing against the sides of holes, a condition encountered with gimbal-mounted bearings. The test was performed in a bath of molten salt 107 for 1000 hr under a load of 200 lb_f. Examination of the test pieces revealed no evidence of self-welding. A similar test will be performed at 1500°F.

Friction Tests on INOR-8

Friction tests were performed at MIT[1] on INOR-8 rubbing against INOR-8 and on INOR-8 against stainless steel. Four tests were performed, each of

[1]E. Rabinowicz.

which covered a temperature range of 70 to 1830°F. The relation between the coefficient of friction and temperature is shown in Fig. 1.1.3. Note that in each test the coefficient drops off over the range of 700 to 900°F and then, in general, remains at approximately 0.25 on up to 1830°F.

Mechanical Seals for Pumps

The modified Fulton Sylphon bellows-mounted seal,[2] undergoing test in a PKP type of centrifugal pump, has accumulated an additional 3048 hr of operation since the previous report period, for a total of 17,878 hr. The pump continues to operate at constant conditions of 1200°F loop temperature, 2400-rpm shaft speed, and 1200-gpm NaK flow. The seal leakage in both the test seal and the Durametallic upper seal has been negligible. The pump was stopped once to check the drive-motor brushes.

MF Performance Loop

An MF type of centrifugal pump has continued in operation[2] and has logged more than 20,000 hr of continuous operation. Since the previous report period the pump has continued operation in a region of cavitation at 2700 rpm, 645 gpm, and 2.5 psig pump-tank cover gas pressure in molten

[2]MSR Quar. Prog. Rep. July 31, 1959, ORNL-2799, p 19.

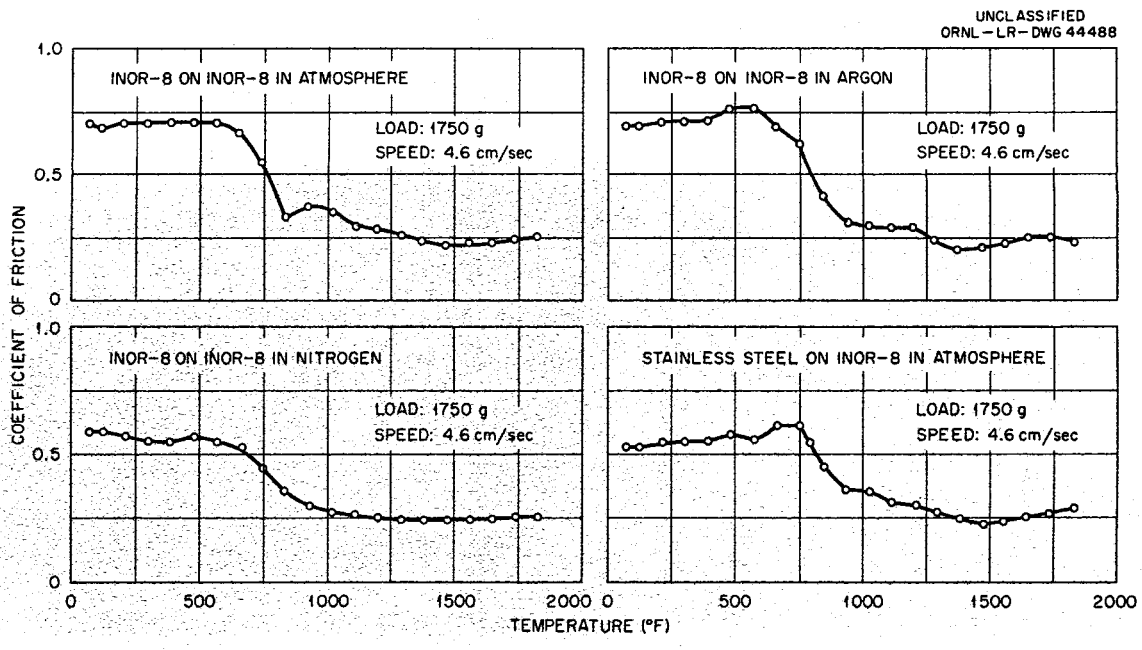

Fig. 1.1.3. Coefficient of Friction vs Temperature for INOR-8 Against INOR-8 and for INOR-8 Against Stainless Steel.

salt 30 at 1200°F. During the quarter the pump was stopped twice – once to replace the air filter on the motor-generator set and once (for 10 min) to replace the brushes in the d-c drive motor. The pump upper- and lower-seal leakage rates have averaged approximately 30 and 12 cc/day, respectively.

Frozen-Lead Pump Seal

The small frozen-lead pump seal being tested on a 3/16-in.-dia shaft, as described previously,[3] has operated continuously since the start of its operation on June 13, 1958. The accumulated operating time, as of October 31, 1959, was 12,000 hr. There was slight leakage of lead during the first 100 hr of operation; there has been no further leakage.

Testing of the large frozen-lead pump seal was discontinued.

Remote Maintenance Demonstration Facility

Construction of the equipment in the Remote Maintenance Demonstration Facility was completed during July. The entire loop of piping (made of 3-1/2- and 6-in. Inconel pipes) was stress-relieved at 1500°F for 2 hr. A check of torque settings on the bolts of the freeze flanges after the stress-relieving operation revealed that all suffered loss of tightness; in some instances the bolt torque was reduced to as little as 40% of the original setting. To assure constant bolt torque on the freeze flange joints during thermal cycling, the use of disk springs was suggested. Three sets of Bellville-type springs are presently being tested for this application.

A system of controlling the air flow to the cooling passages of the freeze flanges was designed, and construction drawings were completed. It is believed that such a flow control will eliminate the adverse effects of the differential thermal expansion between the Inconel flanges and copper seal rings and will improve the gas-tightness of the system during thermal cyclings.

The loop was tested for vacuum-tightness with the flange bolts tightened to their original setting after stress-relieving. A pressure rise of 52 μ was recorded in a 56-hr period with the loop isolated. The system was originally evacuated to 17 μ.

---

[3] MSR Quar. Prog. Rep. Oct. 31, 1958, ORNL-2626, p 23.

Television equipment for remote viewing of the cell has been installed. The closed-circuit system consists of four remotely operated cameras. Two of these, equipped with three-lens turrets and used as a stereo pair (Fig. 1.1.4), are mounted on a dolly and are free to travel the whole length of the cell on a rail mounted on top of the control room. The other two, with "auto zoom" lenses, are mounted in other locations of the cell. The complement of cameras allows nearly 90% coverage of the cell. All four cameras feed into a pair of monitors mounted on a stereo viewer above the General Mills manipulator console (Fig. 1.1.5).

The picture quality and equipment reliability were not satisfactory during early operation; however, with the assistance of a factory representative, local maintenance personnel were able to correct most of the difficulties. Upon completion of suggested modifications, the frequency of maintenance on the viewing equipment was reduced, at times, from 1 in 24 hr to 1 in 200 hr of operation.

Remotely viewed operation of the General Mills manipulator and overhead crane was started in September. Tasks successfully executed by remote means to date include removal and installation of the PK salt pump,

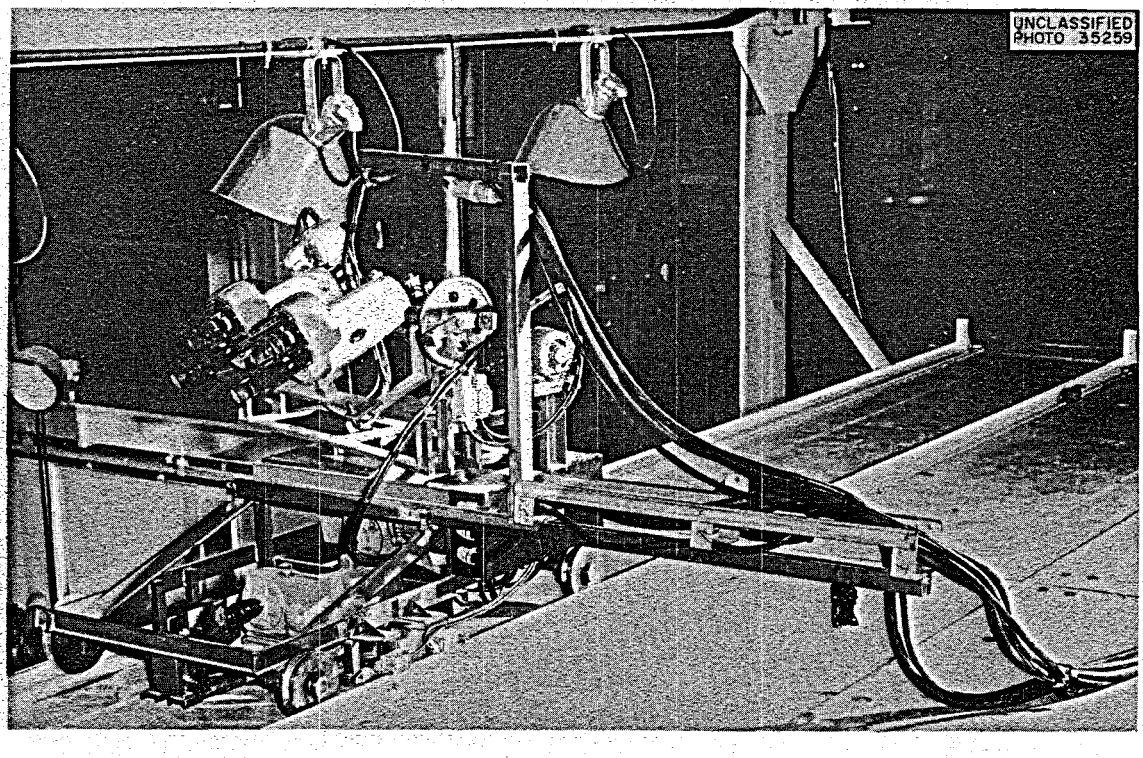

Fig. 1.1.4. Stereo Camera Pair for Viewing Operations in the Remote Maintenance Demonstration Facility.

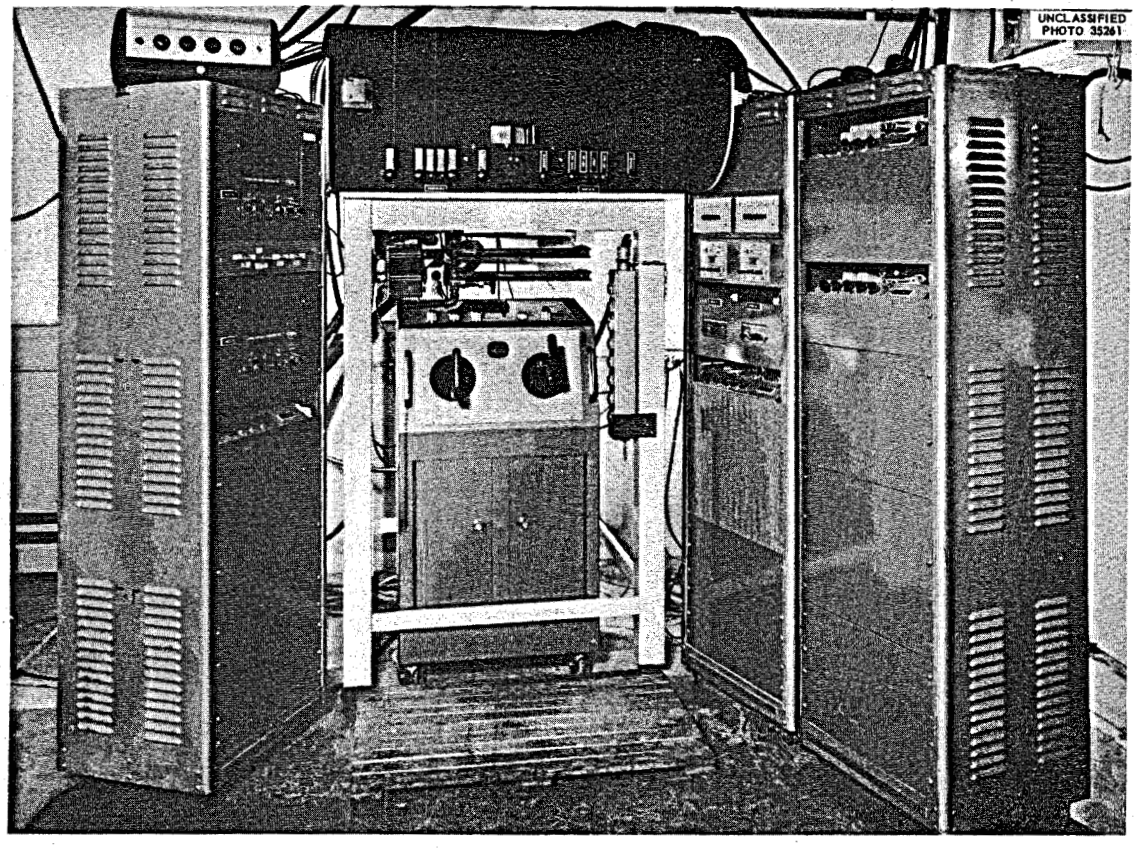

Fig. 1.1.5. Control Center for General Mills Manipulator Console, Closed-Circuit Television, and Overhead Crane; Remote Maintenance Demonstration Facility.

its motor, the dump tank, the freeze valve, the electric heater and insulation unit, and the heat exchanger.

Numerous modifications were incorporated in the loop, as the need arose, either to improve visibility through the cameras or to facilitate maintenance operations. Removal and installation of the heat exchanger, for example, were made practicable by providing guide pins and funnels at the mating flanges and by adding a screw-jack mechanism to close and back away the heat exchanger (Figs. 1.1.6 and 1.1.7).

A variety of tools were fabricated and are in use in conjunction with the overhead crane and the manipulator.

Remote removal of the core vessel is scheduled prior to running molten salt through the loop. Upon completion of the salt run the disassembly-assembly cycle will be repeated on all components.

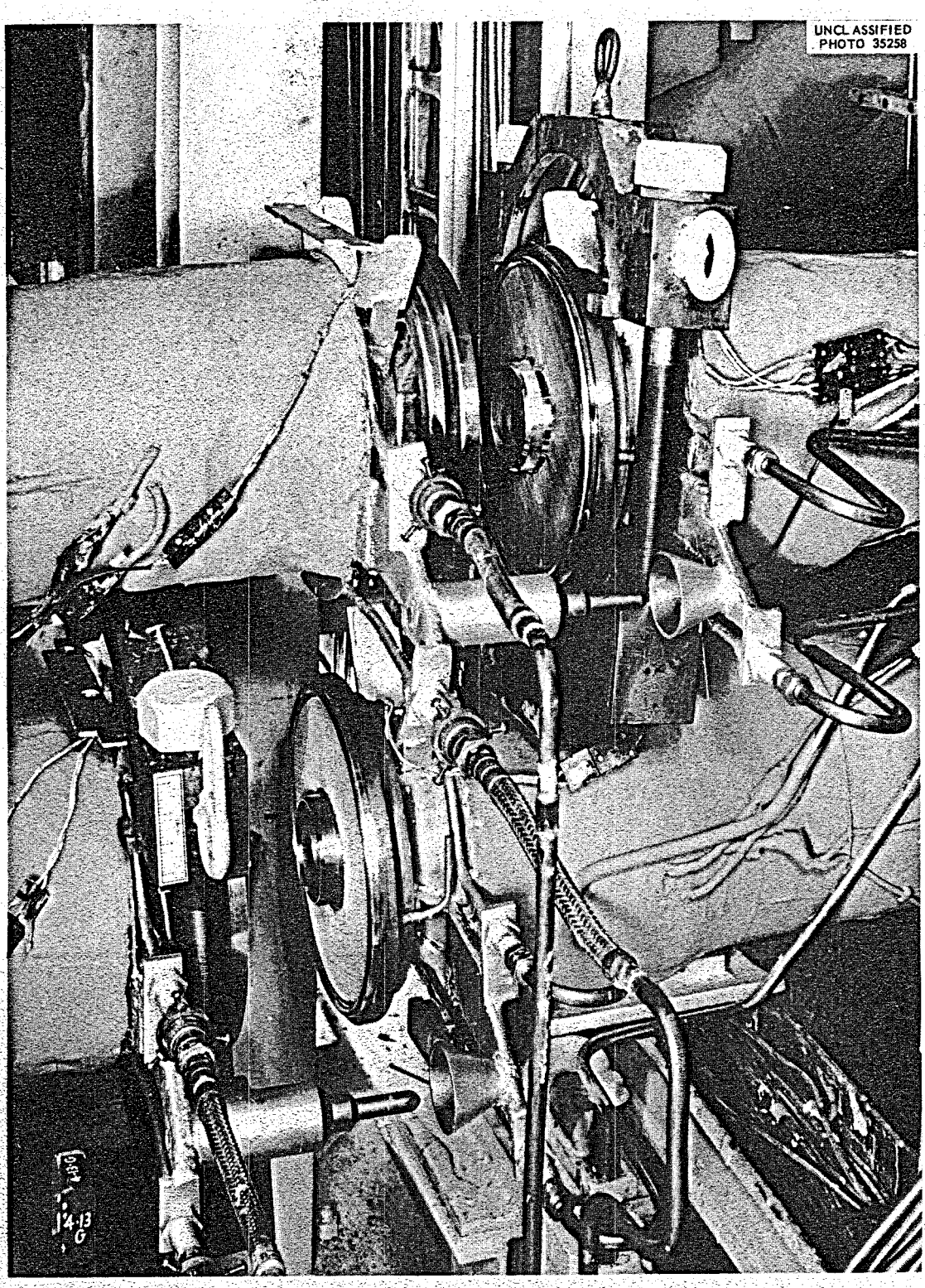

Fig. 1.1.6. Guide Pins and Funnels for Alignment of Flanged Joints in the Remote Maintenance Demonstration Facility.

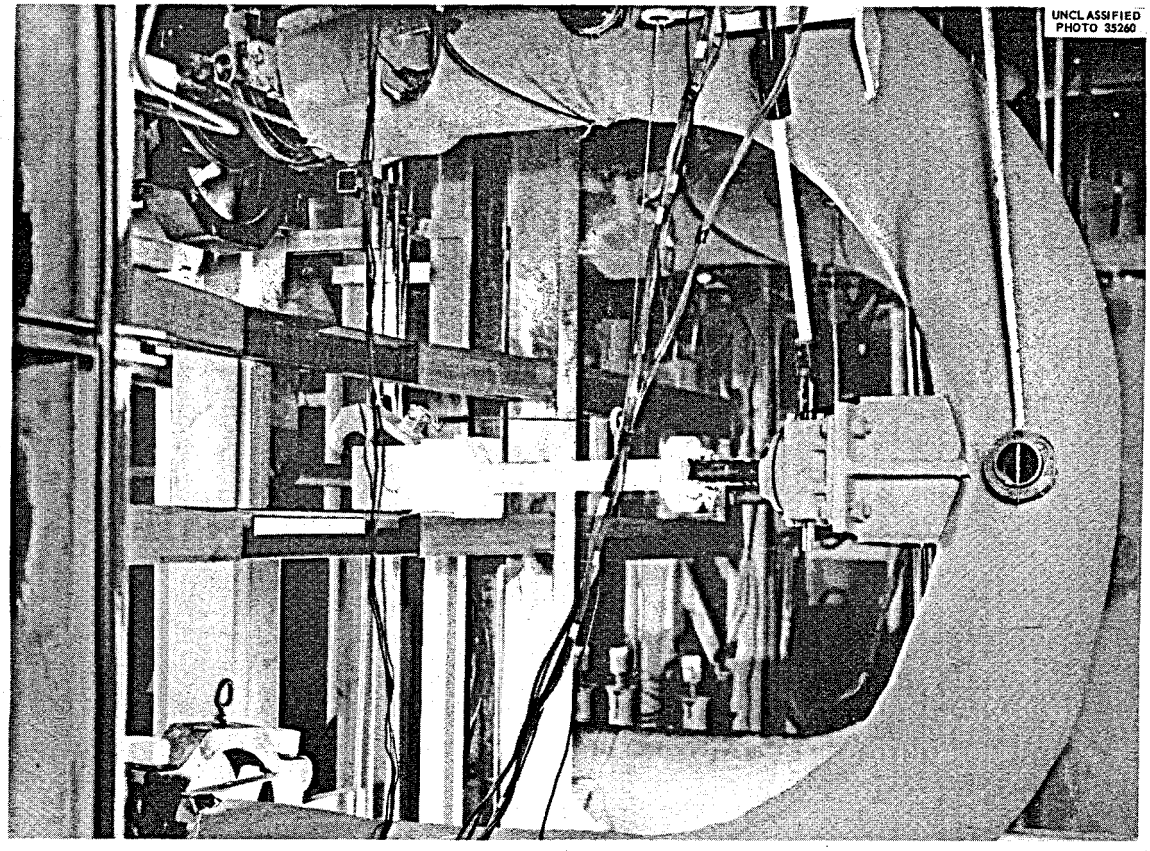

Fig. 1.1.7. Auxiliary Screw Jack for Manipulating the Heat Exchanger in the Remote Maintenance Demonstration Facility.

Design, Construction, and Operation of Materials-Testing Loops

Forced-Circulation Corrosion Loops

The operation of long-term forced-circulation corrosion-testing loops was continued. Table 1.1.2 gives a summary of 16 loop operations during the period, with accumulated hours of operation at test conditions. Eleven of the loops have operated for a full year. (Four other loops with one year of operation had been terminated earlier.[4])

Operation of INOR-8 loops MSRP-8 and -9 and Inconel loop 9377-4 was terminated during this period for metallurgical examination. The two INOR-8 loops had operated without an incident; no dumping or freeze-up of the salt was experienced in the loops although both sustained at least five building-power failures. The LFB pump in the Inconel loop had been

[4]MSR Quar. Prog. Rep. Jan. 31, 1959, ORNL-2684, p 61; Apr. 30, 1959, ORNL-2723, p 33; July 31, 1959, ORNL-2799, p 31.

Table 1.1.2. Molten-Salt Forced-Circulation Corrosion Loops; Operations Summary as of October 31, 1959

Loop	Material	Circulated Fluid*	Operation at Test Conditions (hr)**	Comments
9354-3	INOR-8	84	14,538	Pump has been replaced; loop is awaiting a new batch of salt
9354-1	INOR-8	126	13,746	Normal operation
9354-4	INOR-8	130	10,756	Insert sample No. 2 removed at 10,000 hr; operation resumed
MSRP-7	INOR-8	133	10,534	Tubing sample removed after 1 yr; operation resumed
MSRP-6	INOR-8	134	10,310	Normal operation
MSRP-9	INOR-8	134	9,687	Terminated Oct. 21, 1959
MSRP-8	INOR-8	124	9,633	Terminated Oct. 12, 1959
MSRP-10	INOR-8	135	9,553	Tubing sample removed after 1 yr; operation resumed
9377-4	Inconel	130	9,552	Terminated Sept. 14, 1959
MSRP-11	INOR-8	123	9,344	Normal operation
MSRP-12	INOR-8	134	8,845	Normal operation
9377-5	Inconel	134	8,015	Normal operation
9377-6	Inconel	133	5,830	Normal operation
MSRP-13	INOR-8	136	4,901	Normal operation
MSRP-14	INOR-8	BULT-14	280	Began operation Oct. 14, 1959
MSRP-15	INOR-8	BULT-14	200	Began operation Oct. 23, 1959

*Compositions (mole %):

84	$NaF-LiF-BeF_2$ (27-37-38)	133	$LiF-BeF_2-ThF_4$ (71-16-13)
123	$NaF-BeF_2-UF_4$ (53-46-1)	134	$LiF-BeF_2-ThF_4-UF_4$ (62-36.5-1-0.5)
124	$NaF-BeF_2-ThF_4$ (58-35-7)	135	$NaF-BeF_2-ThF_4-UF_4$ (53-45.5-1-0.5)
126	$LiF-BeF_2-UF_4$ (53-46-1)	136	$LiF-BeF_2-UF_4$ (70-10-20)
130	$LiF-BeF_2-UF_4$ (62-37-1)	BULT-14	$LiF-BeF_2-ThF_4-UF_4$ (67-18.5-14-0.5)

**All tests are operating with a 1300°F high wall temperature and a ΔT of 200°F between high wall and low fluid temperatures, with one exception: MSRP-15 has a high wall temperature of 1400°F.

replaced three times, which required dumping and cooling of the loop. Examination of the loops is in progress.

INOR-8 loop 9354-3 was shut down in September when a pump failure resulted in an oil fire. The pump has been replaced, and operation of the loop will be resumed on receipt of a new batch of salt.

INOR-8 loop 9354-4 was shut down in September, after 10,000 hr of operation, for the removal of the second of three sample inserts[5] contained in the hot leg. Results of the examination of this insert are given in Sec 2.1 of this report. Operation was resumed with the remaining (third) insert.

INOR-8 loops MSRP-7 and -10 were shut down for the removal of tubing sections from the hot leg after 8760 hr (one year) of operation. The sections were replaced and operation was resumed. The sections are now being examined by the Metallurgy Section.

Two new INOR-8 loops, MSRP-14 and -15, were placed in operation with salt BULT-14 in October. Both loops contain molten-salt sampling devices and three jacketed insert sections. The double-walled inserts were placed at the exit of the second resistance-heater section as shown in Fig. 1.1.8. The close-fitting combination of jacket and insert was designed to give the same cross section and flow area as the matching loop tubing. Loop MSRP-14 is operating with a high wall temperature of 1300°F, and MSRP-15 with a high wall temperature of 1400°F.

Graphite-Metal Seal Tests

Several designs for graphite-to-metal frozen-salt seals have been proposed. In the first of the configurations to be tested, the frozen-salt seal will be formed in a narrow annulus between a 5-in.-OD graphite tube and a slightly larger Inconel tube. Such a seal could be used in a molten-salt breeder reactor as the seal between the fuel salt and breeder salt. A sectional view of the test-joint design is shown in Fig. 1.1.9.

Manufacture of parts for the seal-test apparatus is nearly complete, and construction of the test loop has been started. It is expected that the first test of the seal will be made before the end of November 1959.

---

[5]MSR Quar. Prog. Rep. Apr. 30, 1959, ORNL-2723, p 33.

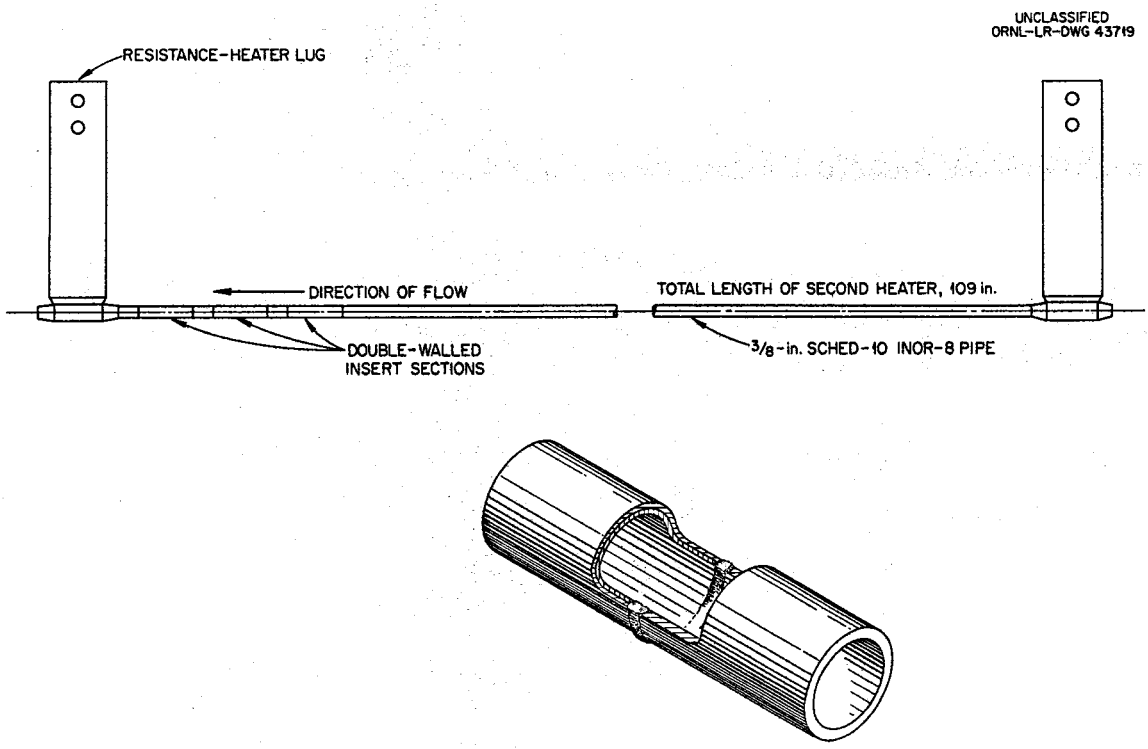

Fig. 1.1.8. Double-Walled Insert Sections Installed in INOR-8 Loops MSRP-14 and -15.

In-Pile Loop

Sectioning and metallographic examination of the first MSR in-pile loop are complete. Analysis of the fuel and of radioactive deposits in the gas passages of the loop is in progress. The second loop has been sectioned, and some preliminary metallographic examination made. The results will be issued after both loops have been examined.

An irradiation program, in conjunction with out-of-pile tests, is under way to study the effects of radiation and fissioning on the properties and fuel penetration of graphite under conditions simulating those of a graphite-core molten-salt reactor. Specimens of promising grades of low-permeability graphite will be submerged in enriched molten-salt fuel under pressure and irradiated in the MTR HB-3 beam hole at 1300°F. A bench test of the irradiation experiment has operated satisfactorily, and the first experiment is scheduled for insertion in the MTR early in 1960.

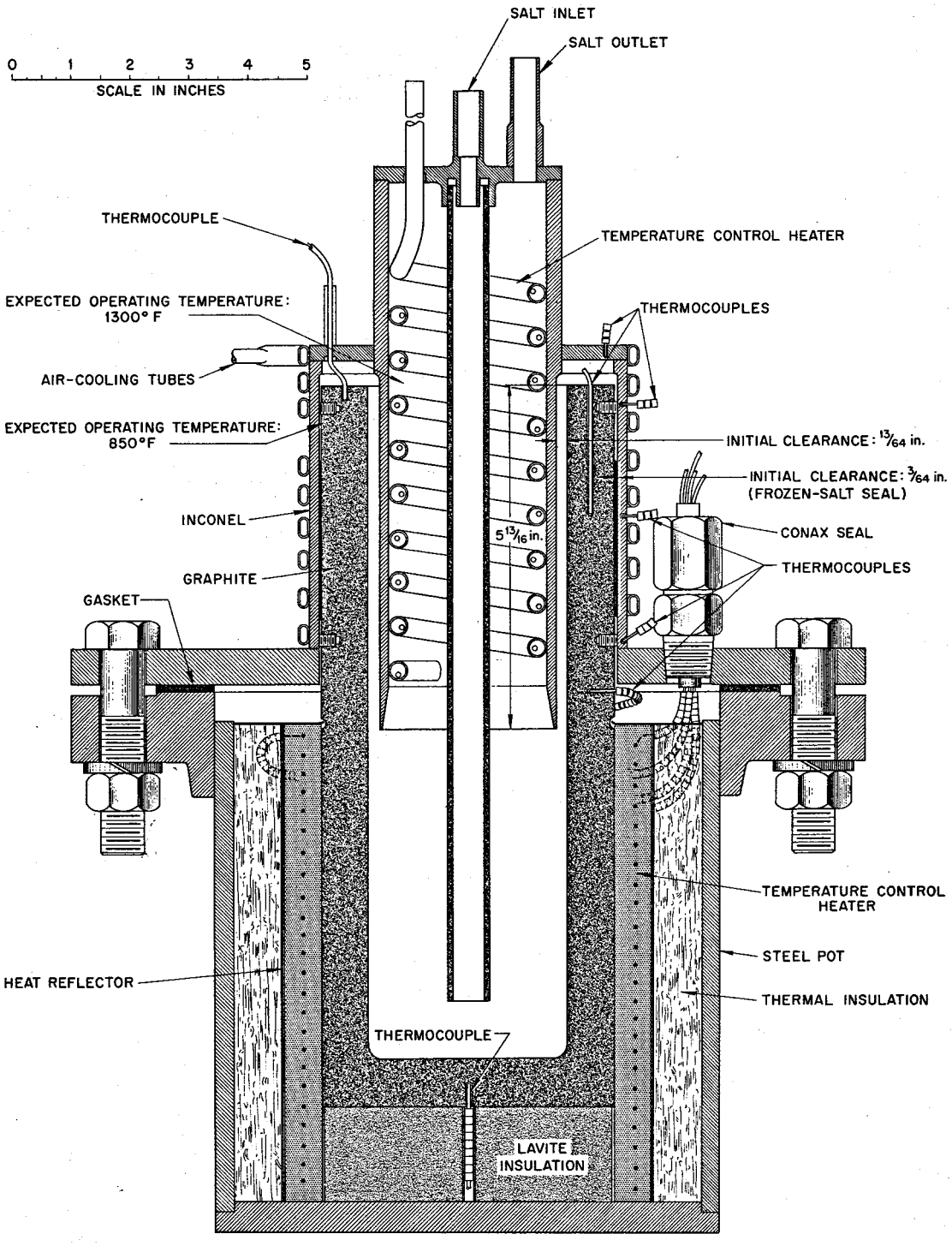

Fig. 1.1.9. Graphite-Metal Freeze-Joint Test Apparatus.

1.2 ENGINEERING RESEARCH

Physical-Property Measurements

Viscosity

The viscosity of the fuel mixture BULT-14 (LiF-BeF_2-UF_4-ThF_4, 67-18.5-0.5-14 mole %) was obtained by using the skirted capillary efflux viscometer.[1] The data from three separate determinations using different viscometer cups are given in Fig. 1.2.1. Also plotted is the correlating line derived by a least-squares analysis of these data; in the temperature range from 550 to 800°C, this analysis yielded the equation

$$\mu = 0.0812e^{4422/T} ,$$

where μ is the viscosity in centipoises and T is the absolute temperature (°K). The viscosity of the BULT-14 mixture is compared in Fig. 1.2.2 with earlier results[1-3] on salts 133 (LiF-BeF_2-ThF_4, 71-16-13 mole %), 134

---

[1] MSR Quar. Prog. Rep. Jan. 31, 1959, ORNL-2684, p 65.
[2] MSR Quar. Prog. Rep. Apr. 30, 1959, ORNL-2723, p 39.
[3] MSR Quar. Prog. Rep. July 31, 1959, ORNL-2799, p 34.

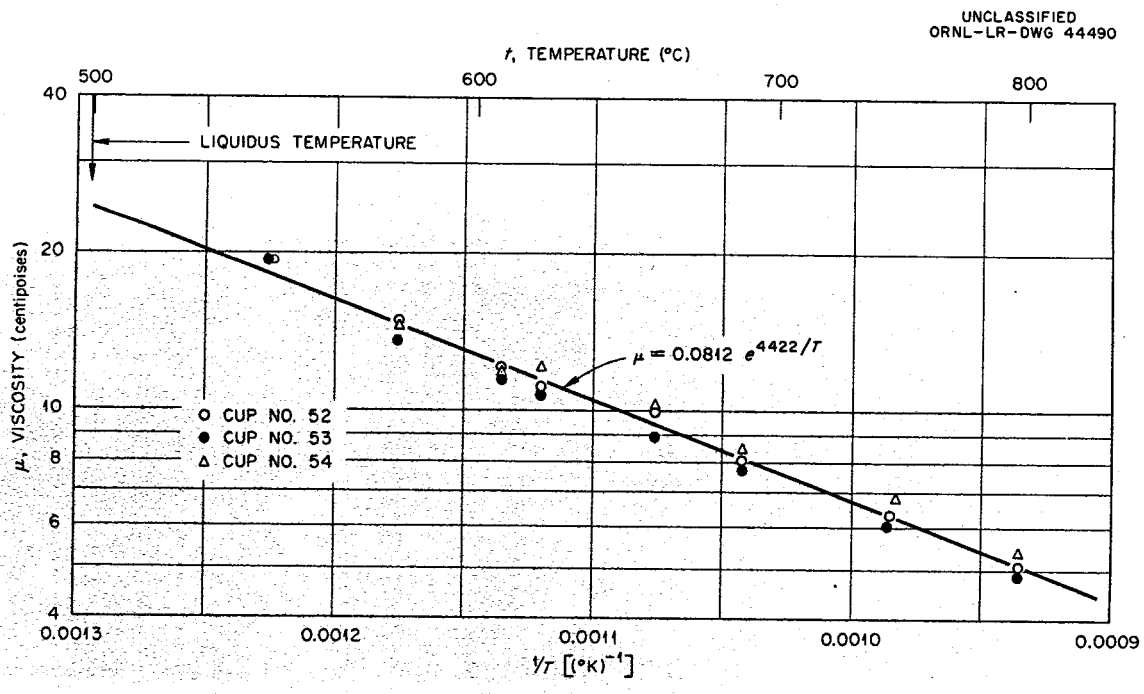

Fig. 1.2.1. Viscosity-Temperature Relationship for the Fuel Mixture BULT-14 (LiF-BeF_2-UF_4-ThF_4, 67-18.5-0.5-14 Mole %).

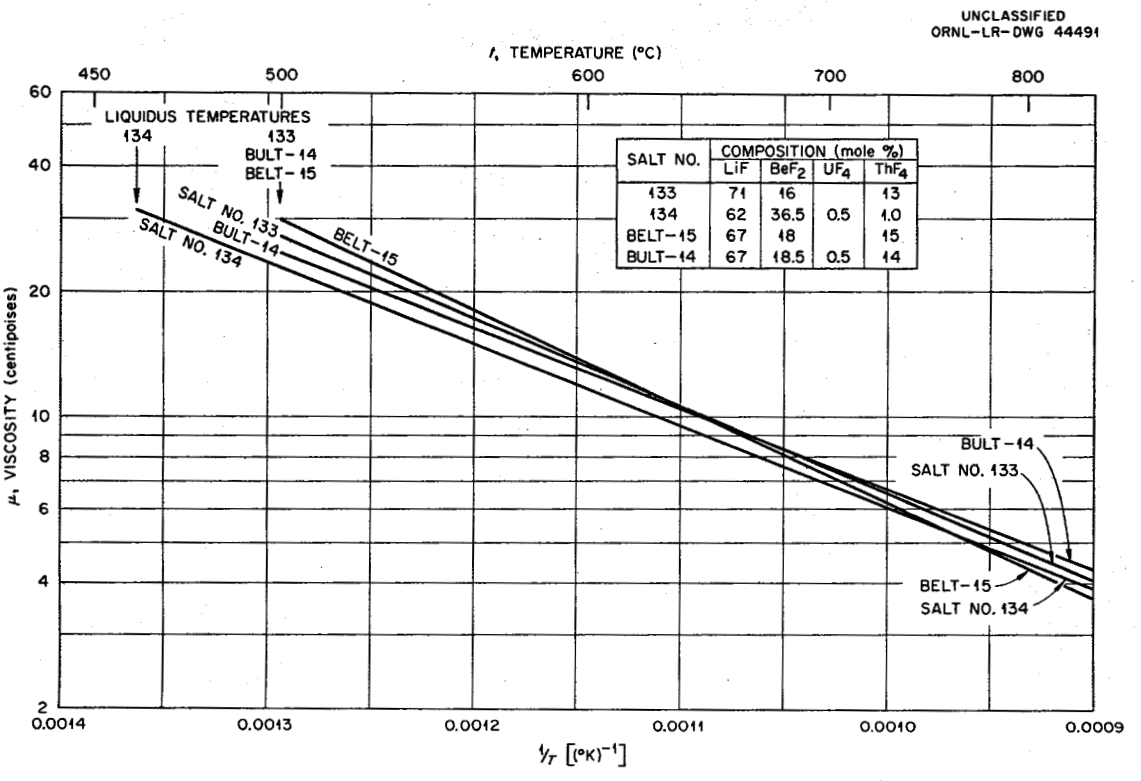

Fig. 1.2.2. A Comparison of the Viscosities of Four Thorium-Containing Molten Salt Mixtures.

($LiF-BeF_2-ThF_4-UF_4$, 62-36.5-1-0.5 mole %), and BeLT-15 ($LiF-BeF_2-ThF_4$, 67-18-15 mole %). The viscosities of the three high-thorium-content salts deviate by a maximum of 18% (at the extremes of the temperature range). This large variation is rather surprising in view of the small composition change between BeLT-15 and BULT-14; the viscosities of these two mixtures will be redetermined in the near future.

Results for the BeF_2-containing salts studied to date are summarized in Table 1.2.1.

Enthalpy and Heat Capacity

Analysis of the previously reported data[4] on the enthalpy of the BeLT-15 mixture was completed. For the solid (100–400°C), the enthalpy (in cal/g) can be expressed as

$$H_t - H_{30} = -6.5 + 0.190t + (5.5 \times 10^{-5})t^2 \quad ,$$

[4] Ibid., p 38.

Table 1.2.1. Viscosities of BeF_2-Containing Salts

Salt No.	Composition (mole %)					Empirical Constants*	
	LiF	NaF	BeF_2	UF_4	ThF_4	A	B
123		53	46	1		0.0234	5505
126	53		46	1		0.0104	6487
130	62		37	1		0.0580	4550
133	71		16		13	0.0526	4838
134	62		36.5	0.5	1	0.0680	4497
136	70		10	20		0.0489	4847
BeLT-15	67		18		15	0.0311	5308
BULT-14	67		18.5	0.5	14	0.0812	4422

*Constants appear in the equation, $\mu = Ae^{B/T}$.

and for the liquid (550–800°C) as

$$H_t - H_{30} = -38.5 + 0.418t - (7.0 \times 10^{-5})t^2 \quad ,$$

where t is the temperature (°C). The heat of fusion at 500°C was determined to be 48 cal/g.

Preliminary data on the enthalpy of the BULT-14 composition are given in Fig. 1.2.3; analysis is continuing.

Thermal Expansion

The apparatus for determining the thermal expansion of molten-salt mixtures is pictured in Figs. 1.2.4 and 1.2.5. This device obtains, as described in an earlier report,[5] the thermal expansion of the liquid by measuring the difference in height of the fluid in the two legs of a U-tube when the legs are maintained at different temperatures. The density at any temperature, t, is expressed as

$$\rho_t = \rho_0[1 - \beta(t - t_0)] \quad ,$$

[5]MSR Quar. Prog. Rep. June 30, 1958, ORNL-2551, p 39.

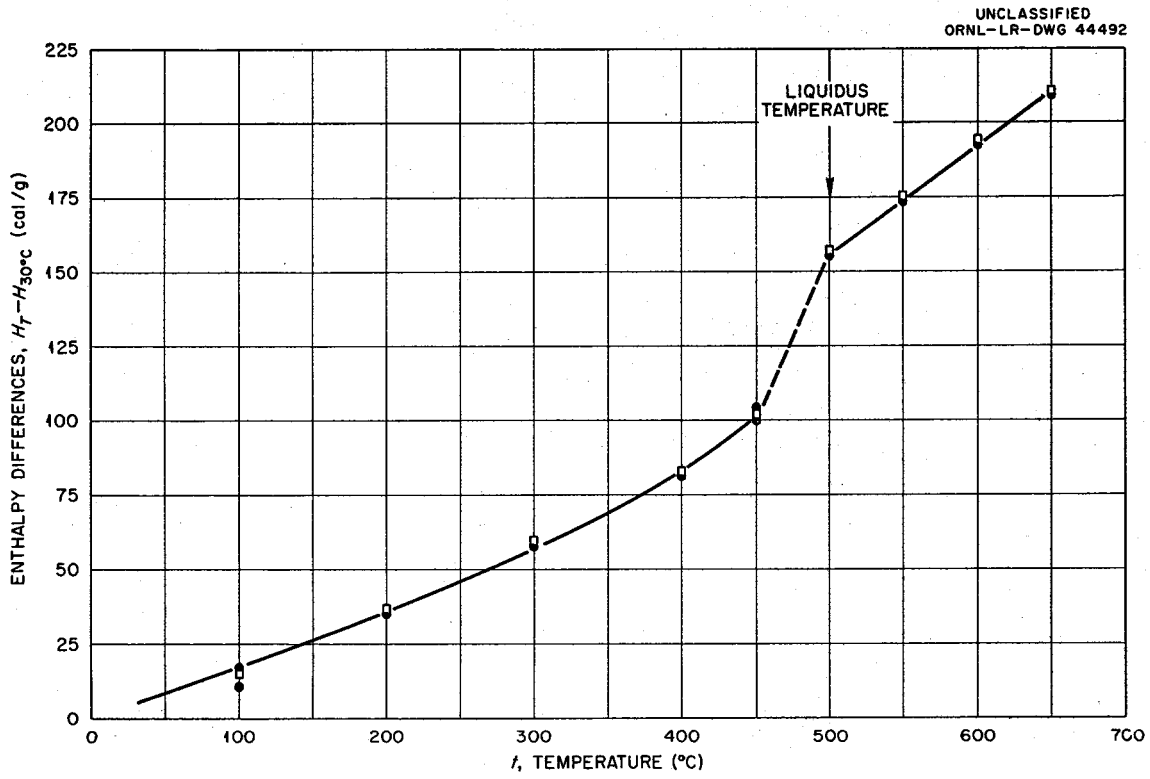

Fig. 1.2.3. Enthalpy-Temperature Relationship for the Fuel Mixture BULT-14 (LiF-BeF_2-UF_4-ThF_4, 67-18.5-0.5-14 Mole %).

where ρ_0 is the density at some base temperature, t_0. The volume coefficient of expansion is thereby obtained, to a close approximation, as

$$\beta = \frac{1}{c + x_1} \frac{d(x_1 - x_2)}{dT} ,$$

where x_1 is the height of the liquid in leg 1 and x_2 is the height of liquid in leg 2, both measured above the arbitrary fixed point of the U-tube height, c (note Fig. 1.2.6); T is the temperature difference (°C) between the two legs. In practice, it was found most convenient to vary the temperature of one leg only, the other being held at some fixed reference temperature.

Experimental data from an operational study of this apparatus using the salt mixture HTS ($NaNO_2$-$NaNO_3$-KNO_3, 40-7-53 wt %) are shown in Fig. 1.2.6. From this figure, the slope, dX/dT (where $X = x_1 - x_2$), was found to be 4.808×10^{-3} in./°C; β is then calculated to be 0.000363 $(g/cm^3) \cdot (g/cm^3)^{-1} \cdot (°C)^{-1}$ (±2%) over the temperature range from 215 to 315°C. This can be compared with the value of β, 0.000378, obtained from density

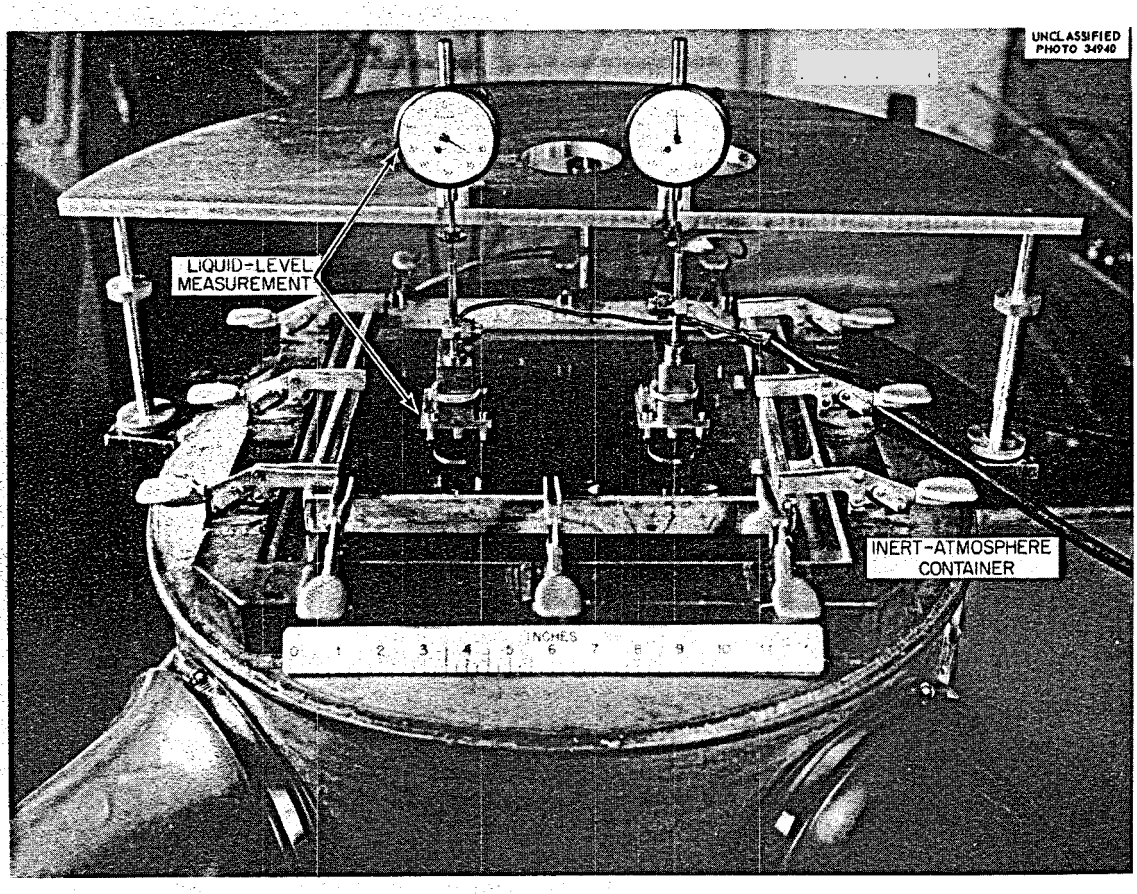

Fig. 1.2.4. Apparatus for Determining Thermal-Expansion Coefficient of Molten Salts.

measurements by Vargaftik et al.[6] Measurements with the BULT-14 mixture were initiated.

Heat-Transfer Studies

Preliminary measurements were made of the heat-transfer coefficients for the salt mixture BULT-14 (LiF-BeF_2-UF_4-ThF 67-18.5-0.5-14 mole %) flowing in heated Inconel and INOR-8 tubes. The apparatus, described in earlier reports,[7] is shown in Figs. 1.2.7 and 1.2.8.

Initial operation of the system was terminated, after 24 hr of circulation at a mean temperature of 1180 to 1195°F, by an internal leak in the heat exchanger. Since it had been observed during this period that

[6]N. B. Vargaftik, B. E. Neimark, and O. N. Oleshchuk," Physical Properties of a Fluid Heat-Carrier for High Temperatures," Izvest. Vsesoyuz. Teplotekh. Inst. im. Feliksa Dzerzhinskogo 21(9), 1-7 (1952).

[7]MSR Quar. Prog. Rep. Apr. 30, 1959, ORNL-2723, p 41; MSR Quar. Prog. Rep. July 31, 1959, ORNL-2799, p 39.

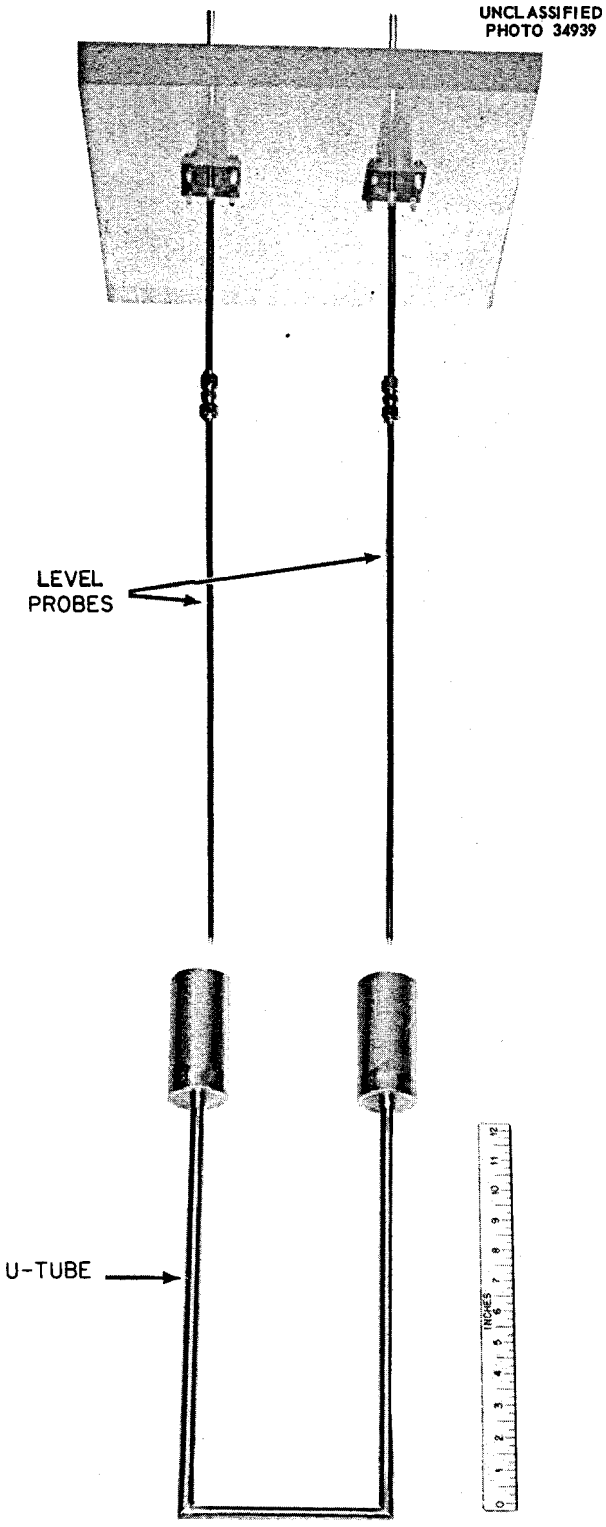

Fig. 1.2.5. Salt Container and Liquid-Level Probes for Thermal-Expansion-Coefficient Apparatus.

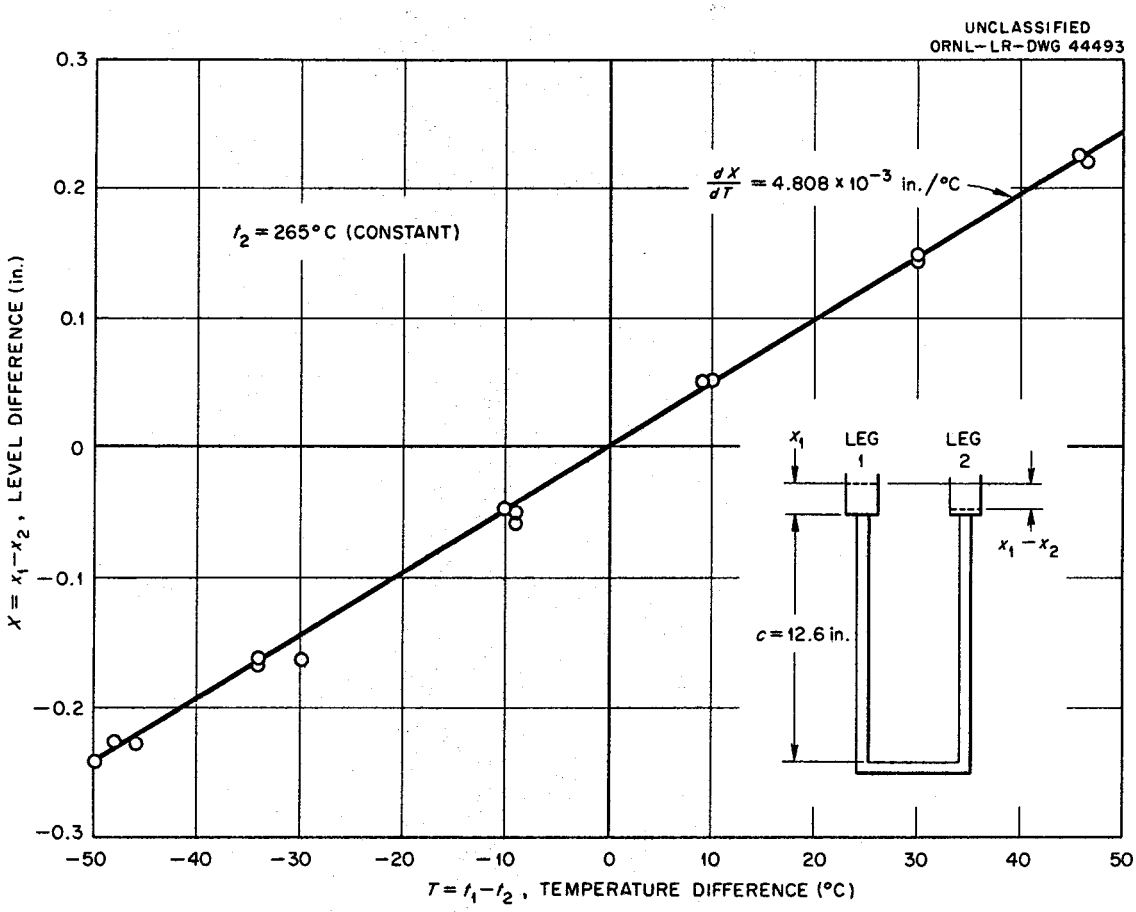

Fig. 1.2.6. Experimental Data for Thermal-Expansion Coefficient of HTS ($NaNO_2$-$NaNO_3$-KNO_3, 40-7-53 wt %).

the heat loss from the piping alone was sufficient to maintain temperatures at the desired levels, the heat exchanger coolant lines were plugged; and circulation was resumed. At higher power levels, partial removal of the thermal insulation in the heat exchanger region satisfied the additional cooling requirements. The system has now operated continuously for some five weeks without difficulty. During this period, Δt runs have been made at regular intervals; normal circulation takes place under isothermal conditions.

Typical axial temperature profiles (outside tube surface) for both the Inconel and INOR-8 sections are shown in Fig. 1.2.9. The tube-wall temperatures have been adjusted to a consistent base by using data from a series of runs in which the power level was set so as to just maintain the salt passing through the test section at its inlet temperature. Under such essentially isothermal conditions, corrections for the tube-wall

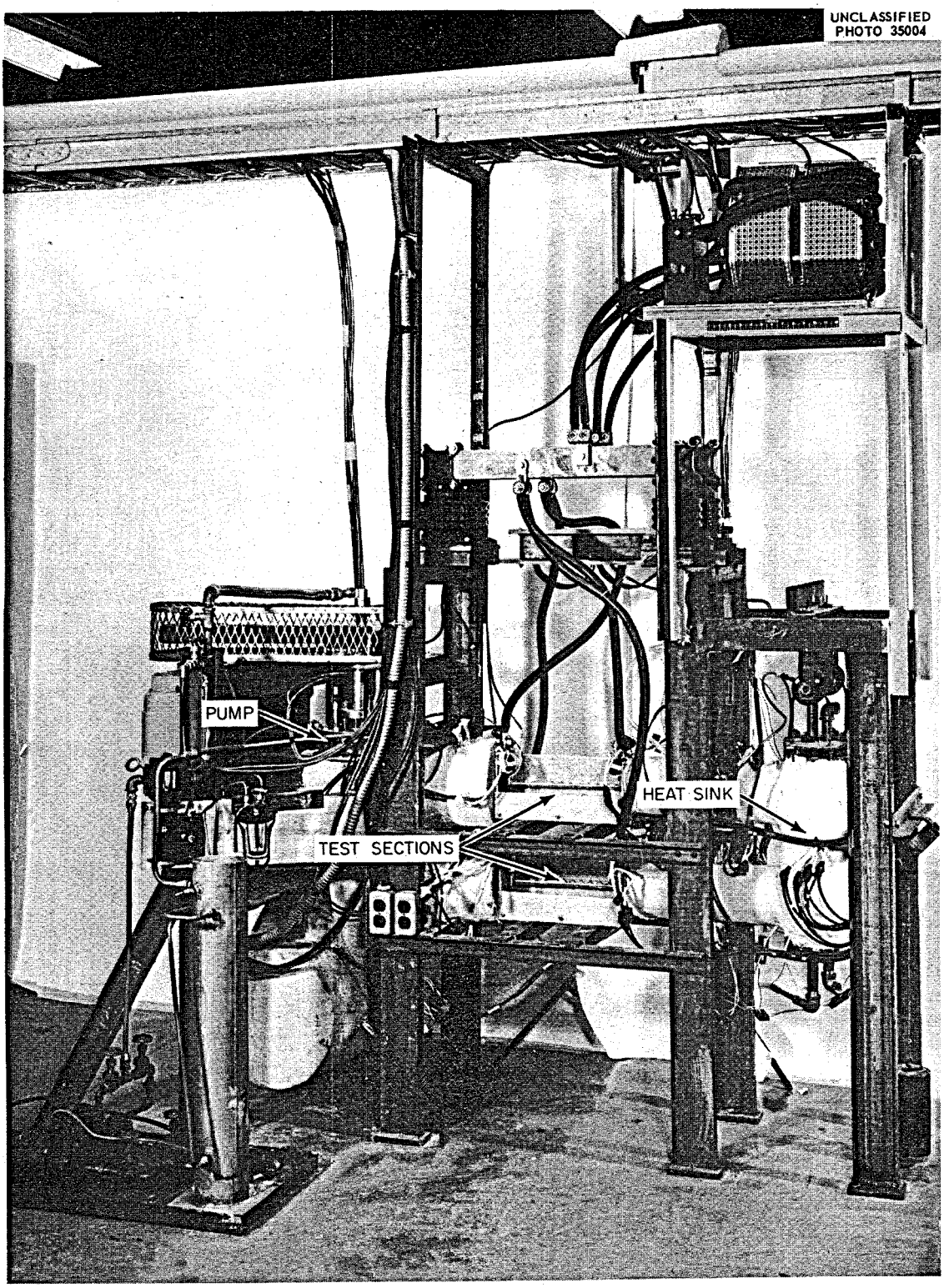

Fig. 1.2.7. Continuous-Circulation System for Study of Heat-Transfer Coefficients with Molten Salts.

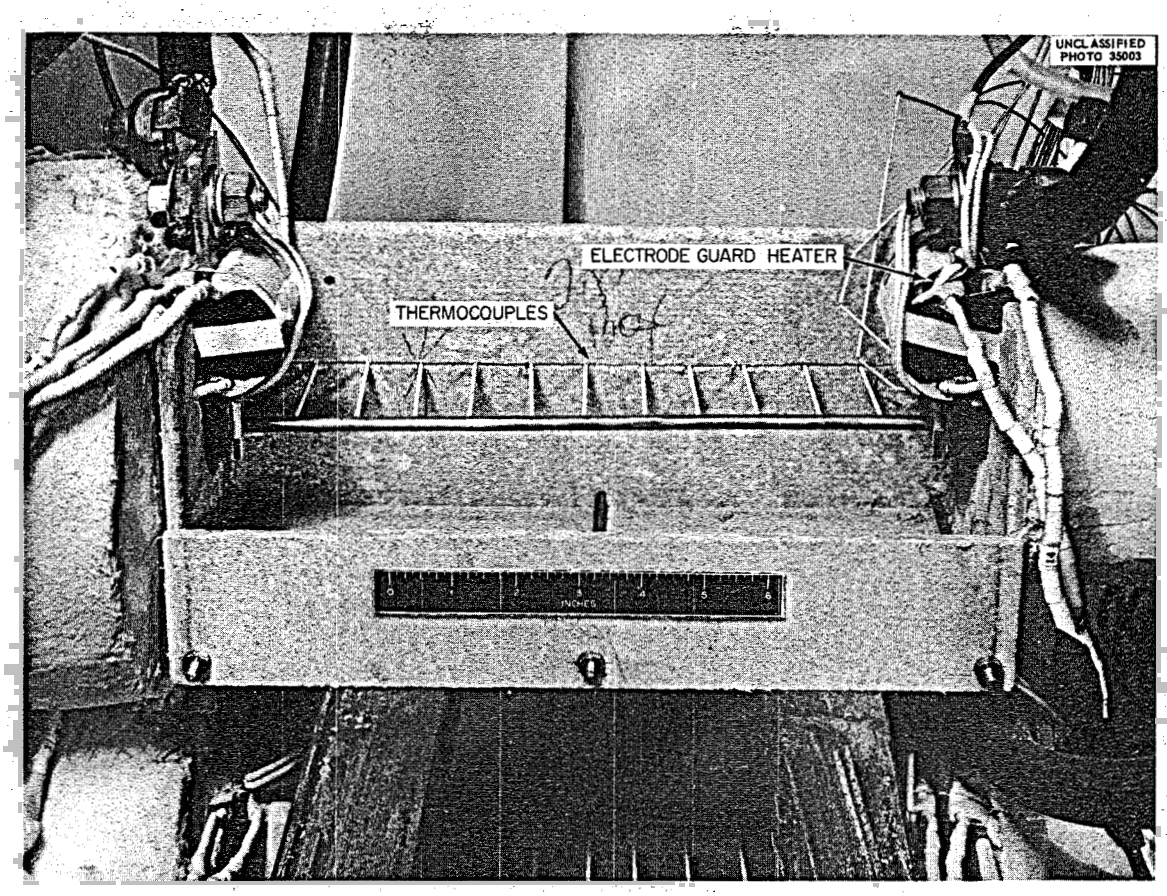

Fig. 1.2.8. Close-up of Inconel Test Section for Study of Molten-Salt Heat Transfer.

thermocouples can be obtained by comparison with the inlet-fluid mixed-mean thermocouple, and the power consumed is a measure of the system heat loss at the operating temperature. Of interest is the unusual shape of the tube-wall temperature profiles of Fig. 1.2.9. Since the fluid enters the test section directly from the larger-diameter mixing chamber and heating occurs over the entire length of the test section, the entrance condition is complicated by the concurrent development of the thermal and hydrodynamic boundary layers. The peaks in the temperature curves can then probably be explained in terms of a laminar-to-turbulent transition in the hydrodynamic boundary layer. Linke and Kunze,[8] studying heat transfer in the entrance region of tubes with the simultaneous development of the flow and temperature fields, found a similar dip in the heat-transfer coefficient (corresponding to a peak in the temperature) in the

[8]W. Linke and H. Kunze, Allgem. Wärmetech. 4, 73–79 (1953); see also E. R. G. Eckert and R. M. Drake, Heat and Mass Transfer, p 213, McGraw-Hill, 1959.

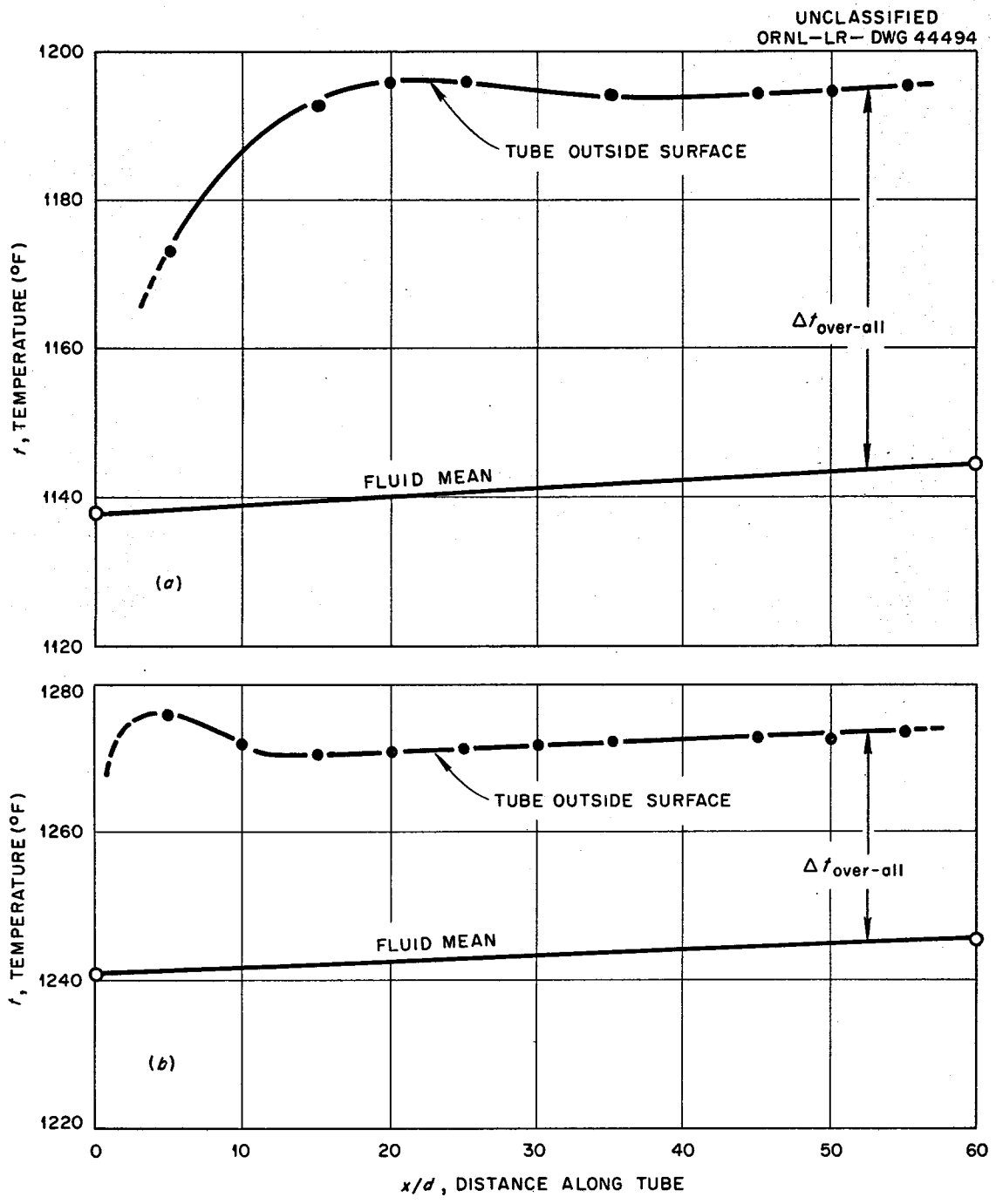

Fig. 1.2.9. Typical Axial Temperature Profiles as Obtained in the Study of the Heat-Transfer Characteristics of an $LiF-BeF_2-UF_4-ThF_4$ (67-18.5-0.5-14 Mole %) Salt Mixture. (a) Run MA-2, Inconel section, $N_{Re} = 7980$; (b) run MA-13, INOR-8 section, $N_{Re} = 13,940$.

vicinity of x/d = 10. Further, the location of this temperature peak should be related to the configuration of the tube entrance in that the transition should occur farther downstream for a rounded entrance than for a sharp-edged entrance. This may explain the shift in the location of the peak between the curves a and b of Fig. 1.2.9; this same difference between the temperature patterns in the Inconel and INOR-8 sections has been observed in all runs made to date. Although a sharp-edged entrance was specified for both sections, welding of the thin-walled tubes into the heating lugs (mixing-chamber end plates) may have altered this situation. Thus it is not possible at this time to define exactly the entrance configuration. Far downstream (x/d > 40) the temperature curves assume the character observed in earlier studies with molten salts[9] under similar conditions of uniform heat input at the wall and established flow and temperature fields.

The results obtained to date are summarized in Fig. 1.2.10 in terms of the heat-transfer parameter, $N_{Nu} \cdot N_{Pr}^{-0.4}$. The wall-to-fluid temperature difference used in the analysis of the data was taken in the region of fully developed conditions (as indicated in Fig. 1.2.9). The heat flux was based on the heat gained by the fluid in passing through the test section; heat balances (corrected for external heat loss) ranged from 0.9 to 1.2. The data are compared in Fig. 1.2.10 with the general heat-transfer correlation[10] for normal fluids under moderate Δt conditions,

$$N_{Nu} = 0.023\ N_{Re}^{0.8}\ N_{Pr}^{0.4} \quad ;$$

also shown are earlier results[11,12] with Flinak (LiF-NaF-KF, 11.5-42-46.5 mole %) and fuel mixtures 30 ($NaF-ZrF_4-UF_4$, 50-46-4 mole %) and 130 ($LiF-BeF_2-UF_4$, 62-37-1 mole %). The low results with the BULT-14 salt mixture may possibly be attributed to the uncertainty in the value of its thermal

---

[9] H. W. Hoffman, Turbulent Forced Convection Heat Transfer in Circular Tubes Containing Molten Sodium Hydroxide, ORNL-1370 (Oct. 3, 1952).

[10] W. H. McAdams, Heat Transmission, 3d ed., p 219, McGraw-Hill, 1954.

[11] H. W. Hoffman, Molten Salt Heat Transfer, ORNL CF-58-2-40 (Feb. 18, 1958).

[12] J. C. Amos, R. E. MacPherson, and R. L. Senn, Preliminary Report of Fused Salt Mixture No. 130 Heat Transfer Coefficient Test, ORNL CF-58-4-23 (Apr. 2, 1958).

conductivity, which was assumed to be 1.3 $Btu \cdot hr^{-1} \cdot ft^{-1} \cdot (°F)^{-1}$ in estimating the heat-transfer parameter. It is planned to determine experimentally the thermal conductivity of the BULT-14 mixture in the near future. The discrepancy observed between the Inconel and INOR-8 data (approximately 23% at N_{Re} = 10,000) is not explainable at present.

Future data, obtained at periodic intervals, will serve to establish whether there exists a progressive film formation for the BULT-14 salt in contact with Inconel or INOR-8.

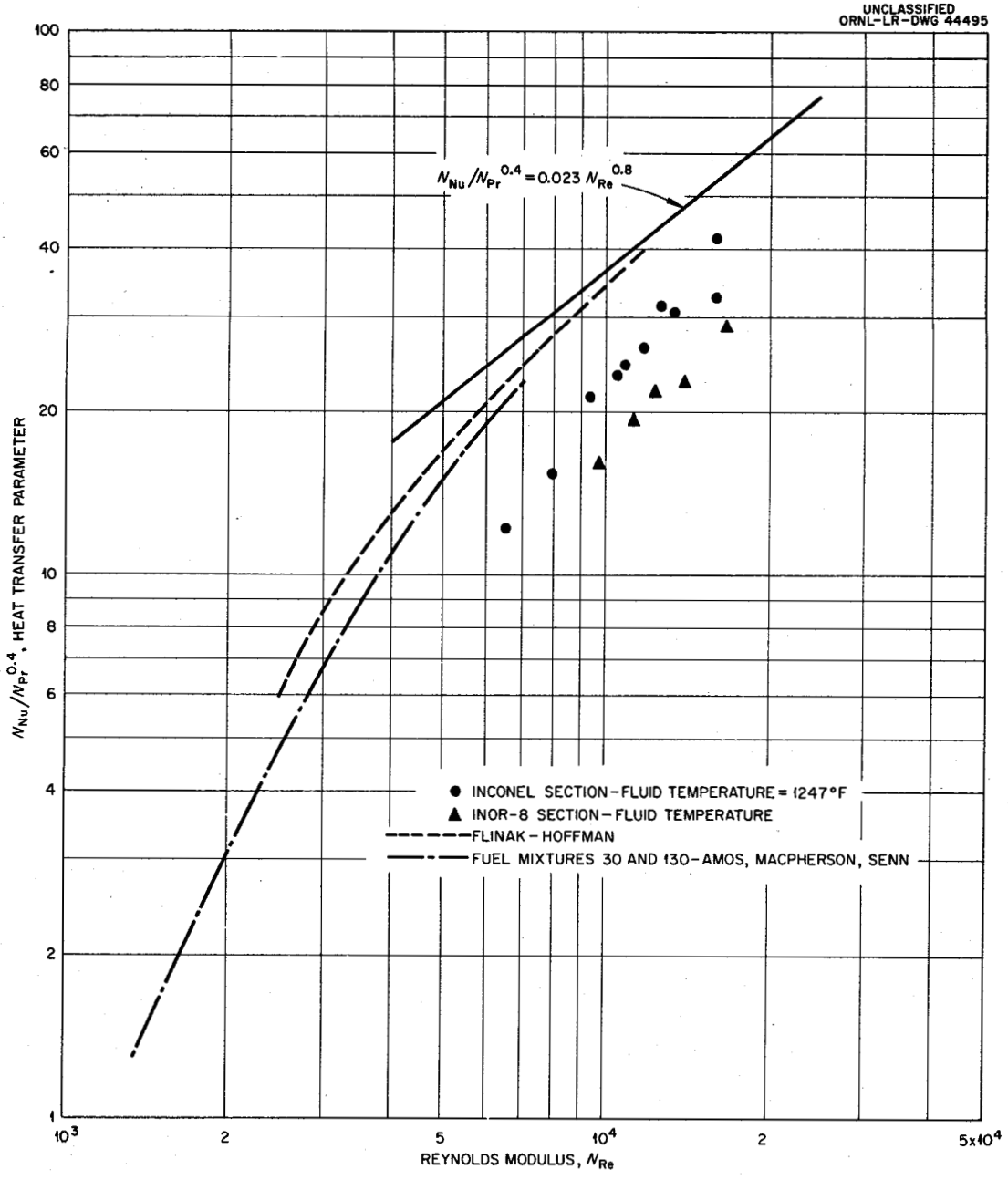

Fig. 1.2.10. Experimental Results for Heat Transfer with BULT-14 Salt Mixture (LiF-BeF_2-UF_4-ThF_4, 67-18.5-0.5-14 Mole %).

PART 2.

MATERIALS STUDIES

2.1 METALLURGY

Graphite Brazing Studies

Graphite has been proposed for use as the moderator of a molten-salt reactor. This material could be placed in the core in simple shapes or as a complex structure such as a heat exchanger that would form a section of the primary loop system. The latter case would probably require graphite-to-graphite and graphite-to-metal joints that have structural integrity and, to an extent, leak-tightness.

A program has consequently been initiated to investigate various techniques for producing joints with graphite and to evaluate their usefulness for molten-salt-reactor service. A preliminary literature survey revealed a notable scarcity of joining techniques applicable to high-temperature-reactor technology. Procedures for wetting graphite are relatively well known, but experience in producing reliable joints in complex assemblies is lacking. One serious problem is related to the gross differences between the thermal-expansion coefficient of graphite and those of common brazing alloys and structural materials.

Metals having a strong tendency to form carbides wet graphite readily when they are molten. Therefore, alloys containing these carbide-forming metals appear promising as brazing alloys for joining graphite to itself and to metals. Zirconium and titanium appear especially attractive, since their thermal-expansion coefficients are relatively low (see Table 2.1.1) and since their melting points can be reduced significantly by only small additions of other elements.

Several brazing alloys containing zirconium and titanium as the major constituents have been developed for the joining of refractory metals. Many of these alloys appear promising for the joining of graphite, but one alloy in particular (48% Ti–48% Zr–4% Be) exhibits excellent flowability. An inverted T-joint made from type AGOT graphite and brazed with this alloy is shown in Fig. 2.1.1. A photomicrograph illustrating the excellent filleting and bonding observed in this joint is shown in Fig. 2.1.2. Figure 2.1.3 illustrates the good flowability obtained by brazing, with this alloy, a low-permeability graphite pipe to a type AGOT graphite sheet.

Brazed joints made with this alloy appear to possess good strength and seem promising for a variety of high-temperature-reactor applications.

Table 2.1.1. Thermal-Expansion Coefficients of Various Materials

Material	Thermal-Expansion Coefficient [μin.·in.$^{-1}$·(°F)$^{-1}$]	Temperature Range (°F)
Graphite	2–3[a]	32–1800
Titanium	4.5[b]	Room
Zirconium	2.8[b]	Room
Molybdenum	2.7[b]	Room
Inconel	10.5[c]	32–1400
Type 430 stainless steel	6.3[b]	32–1500
INOR-8	8.3[d]	32–1800

[a] The Industrial Graphite Engineering Handbook, National Carbon Company.

[b] Metals Handbook.

[c] Engineering Properties of Inconel and Inconel X, International Nickel Company.

[d] Design Data for INOR-8 Alloy, Metallurgy Division, ORNL.

For molten-salt service, however, the uses of this particular alloy are limited by its poor resistance to corrosion in this medium (see "Brazing Material Evaluation in Fuel 130," this section).

This development of other brazing-alloy systems is therefore being undertaken in an effort to find more compatible materials. Utilizing niobium, tantalum, and molybdenum as the primary carbide-forming elements, a number of alloy systems are being studied in detail to determine their applicability for joining graphite. Alloys in the Au-Ni-Ta system have indicated promising wetting characteristics, and several alloy compositions from the gold-rich corner of the ternary diagram have been selected for further study. The relatively high thermal-expansion coefficients of gold-rich alloys, however, may limit their use for joining graphite. Other alloy systems which will be investigated include Ni-Mo, Ni-Nb, Ni-Nb-Mo, Ni-Nb-Ta, Pd-Ni-Ta, and Pd-Ni-Mo.

Preliminary experiments have also been undertaken to determine the feasibility of electric-resistance bonding of graphite to graphite, using molybdenum as the braze metal. So far, experiments have been confined to

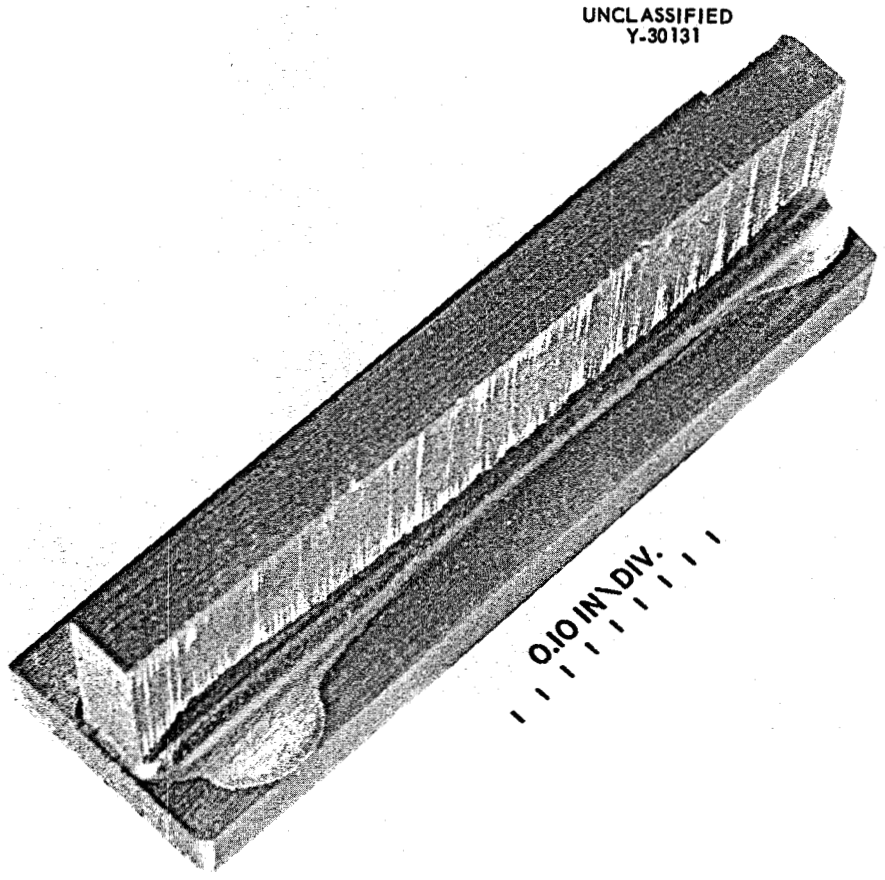

Fig. 2.1.1. Graphite T-Joint Brazed with 48% Ti–48% Zr–4% Be. Excellent wetting and flowability are evident.

graphite rods of 1/4-in. diameter, or less, due to the high-amperage requirements of the process. The joint is prepared by placing a thin disk of molybdenum between the ends of two graphite rods. Evaluation of specimens prepared to date indicates that good structural bonds can be made by this technique. Metallographic examination has shown, however, that careful control will be necessary to minimize porosity and inconsistent bonding.

Dynamic-Corrosion Studies

Forced-Convection Loops

Examination of INOR-8 Hot-Leg Inserts from Loop 9354-4. – A second hot-leg insert was removed from INOR-8 forced-convection loop 9354-4 after 10,000 hr of loop operation. As previously discussed,[1] three inserts were

[1]MSR Quar. Prog. Rep. July 31, 1959, ORNL-2799, p 59.

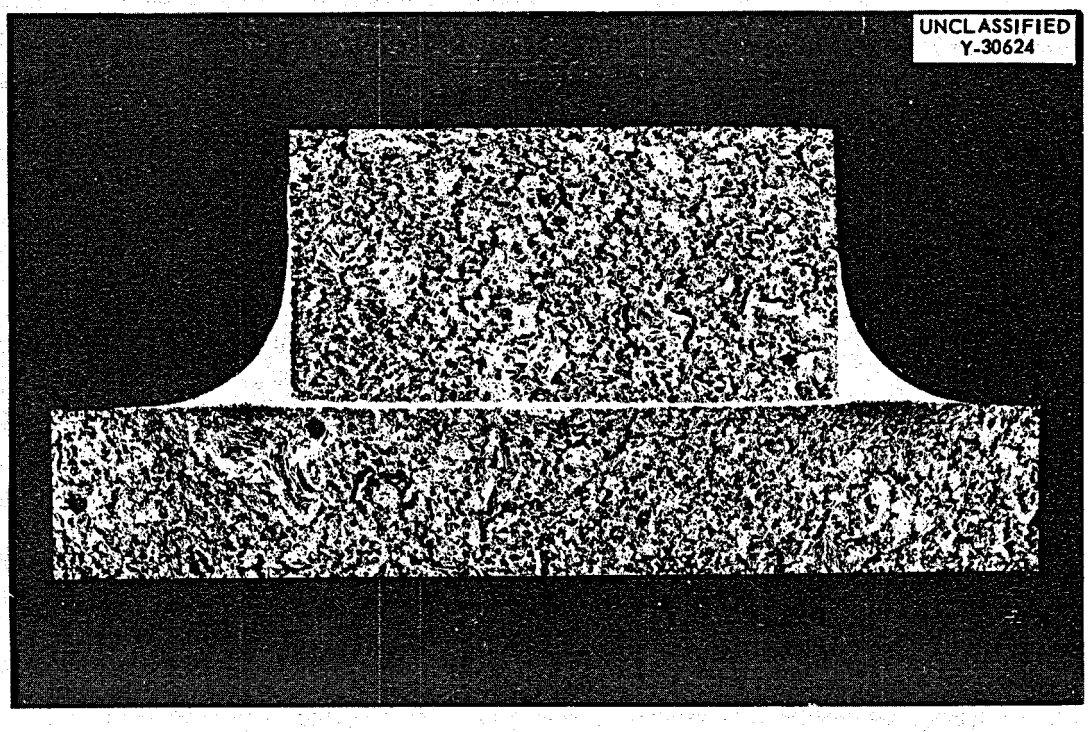

Fig. 2.1.2. Photomicrograph of Graphite T-Joint. As-polished. 12X.

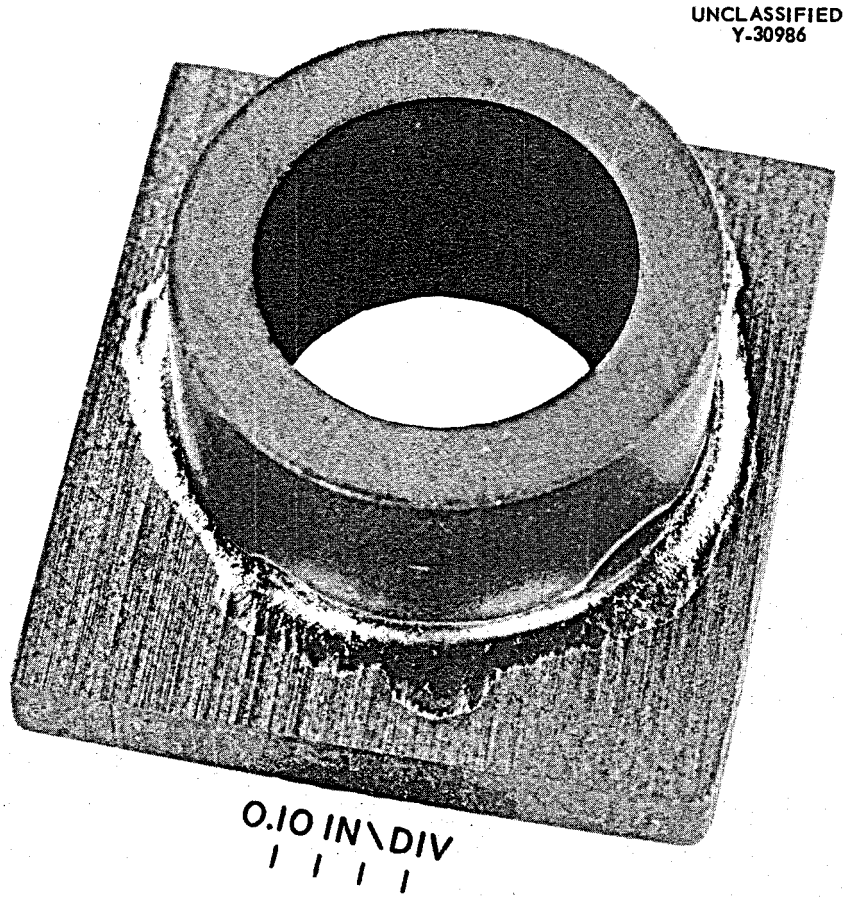

Fig. 2.1.3. Graphite Pipe-to-Sheet Joint Brazed with 48% Ti–48% Zr–4% Be.

installed at the end of the hot-leg section of this loop to provide data on the weight changes of INOR-8 in contact with a beryllium-base fluoride fuel mixture. The schedule specified removal of one insert after 5000 hr of exposure, another after 10,000 hr, and the third after 15,000 hr. Operation of the loop began in July 1958 under the conditions:

Salt mixture	$LiF-BeF_2-UF_4$ (62-37-1 mole %)
Maximum fuel-metal interface temperature	1300°F
Minimum salt temperature	1100°F
ΔT	200°F
Reynolds No.	1600
Flow rate	2 gpm

Examination of the second insert, although not yet complete, indicates that an average weight loss of 2.0 mg/cm^2 (±3%) occurred along its 4-in. length. If uniform removal of surface metal is assumed, this weight loss corresponds to a loss in wall thickness of 0.09 mil. No detectable loss in wall thickness was noted in comparing micrometer measurements of the inserts taken before and after test.

The first of the inserts, which was removed from the loop after 5000 hr, showed a weight loss of 1.8 mg/cm^2 (±2%), or a loss in wall thickness of 0.08 mil. The similarity of these values to the values obtained after 10,000 hr indicates that no significant weight loss occurred after the first 5000 hr of loop operation. The errors listed with these values are based on estimated limits of precision of the instruments used to measure and weigh the insert. They do not include errors resulting from handling of the insert, which are difficult to estimate but could be significant considering the small weight change.

Metallographic examination of transverse and longitudinal sections of the 5000-hr insert revealed light surface roughening, as shown in Figs. 2.1.4 and 2.1.5. Along the exposed edge of the tubing there was evidence of a band between 1 and 2 mils thick containing precipitates and very small grains. The start of a very thin film was also evident along the surface.

Examination of transverse and longitudinal sections of the 10,000-hr insert showed the surface film to have increased in thickness and the band of fine-grained material to have grown in size (Figs. 2.1.6 and 2.1.7).

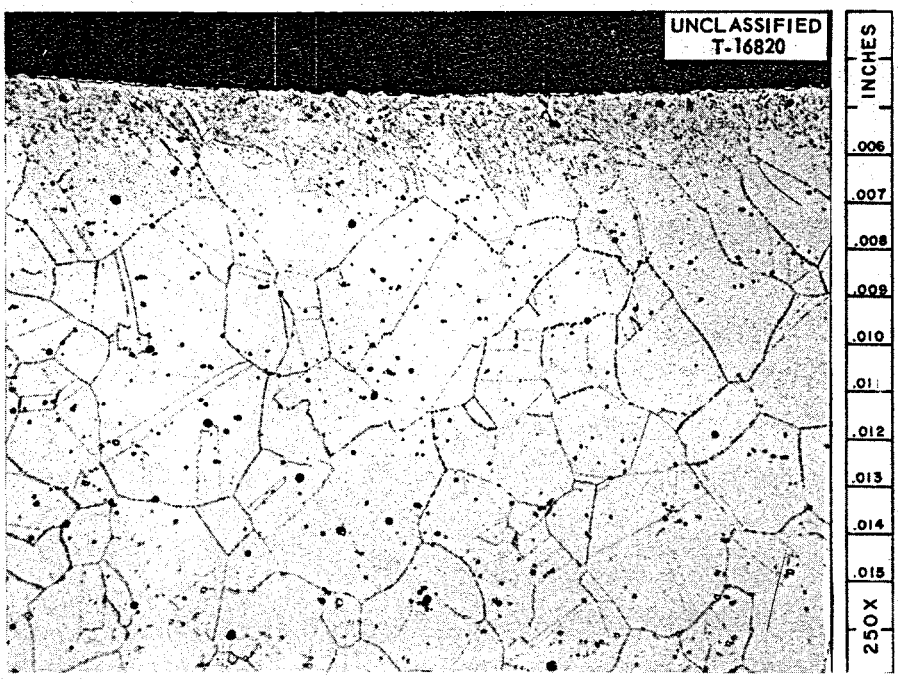

Fig. 2.1.4. Transverse Section of 5000-hr Insert Removed from INOR-8 Pump Loop 9354-4. Etchant: 3 parts HCl, 2 parts H_2O, 1 part 10% chromic acid.

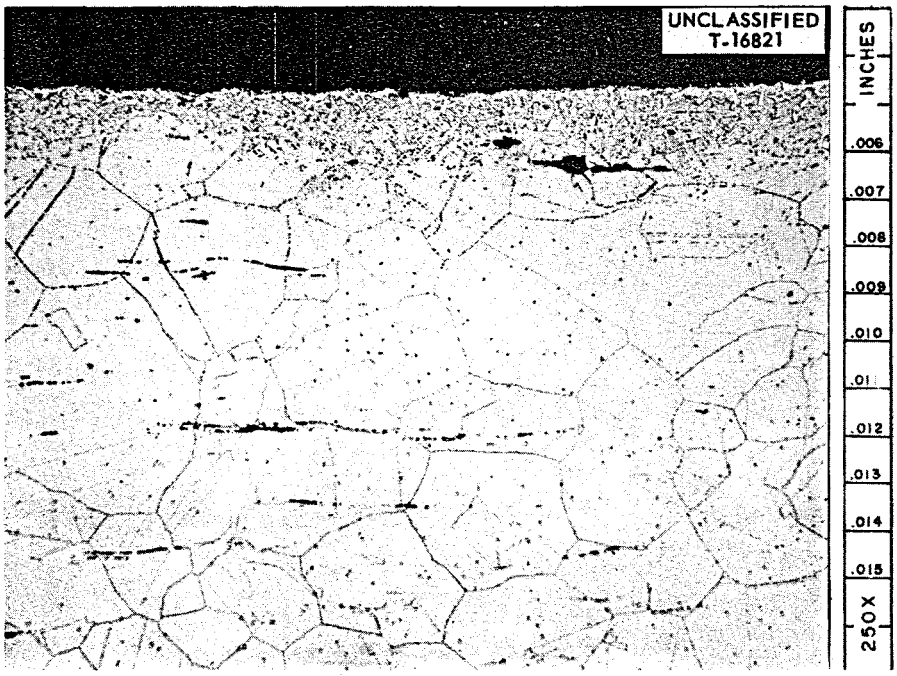

Fig. 2.1.5. Longitudinal Section of 5000-hr Insert Removed from INOR-8 Pump Loop 9354-4. Etchant: 3 parts HCl, 2 parts H_2O, 1 part 10% chromic acid.

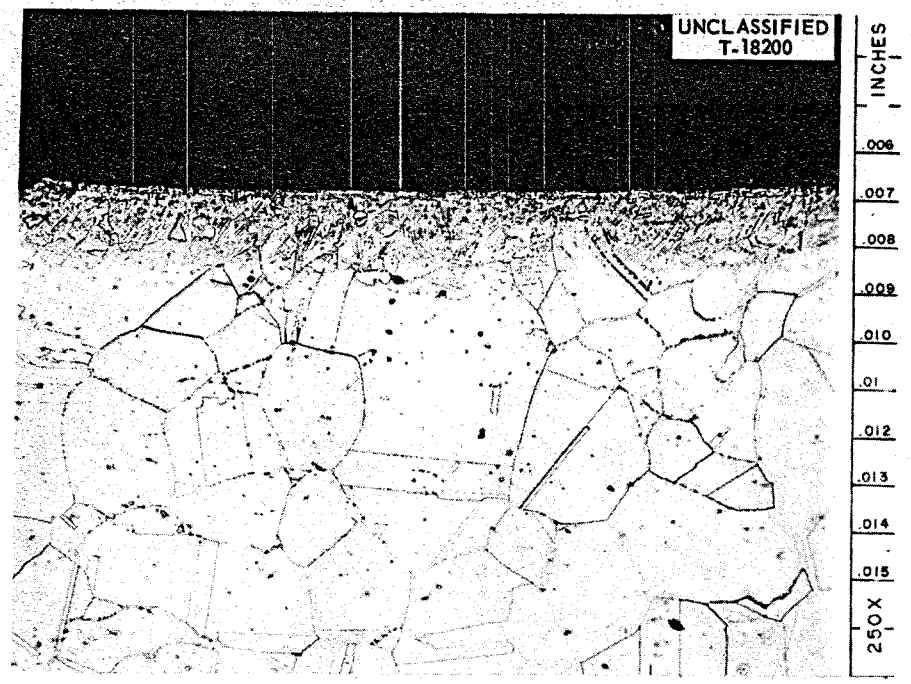

Fig. 2.1.6. Transverse Section of 10,000-hr Insert Removed from INOR-8 Pump Loop 9354-4. Etchant: 3 parts HCl, 2 parts H_2O, 1 part 10% chromic acid.

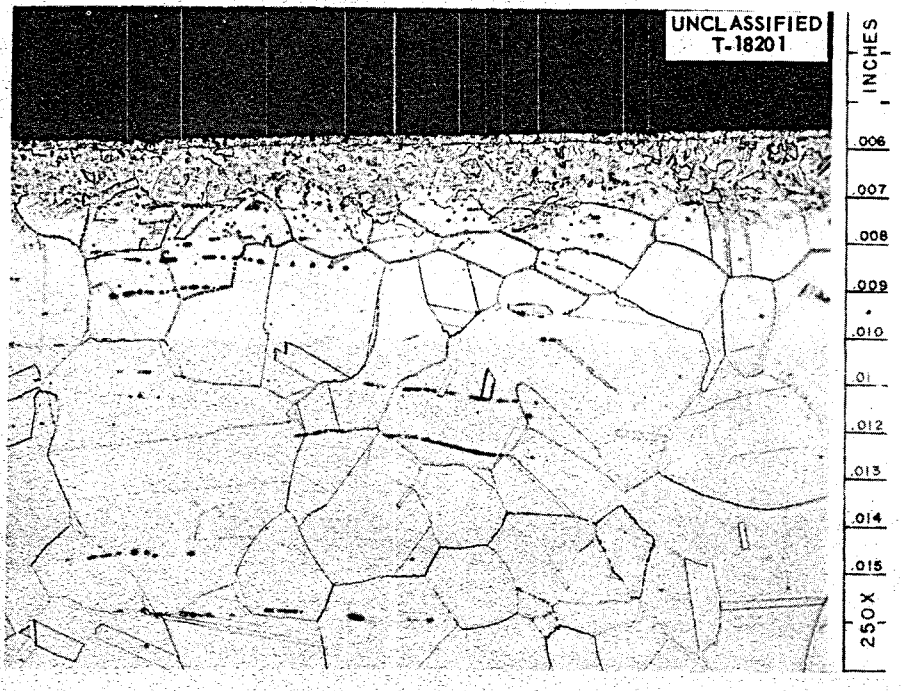

Fig. 2.1.7. Longitudinal Section of 10,000-hr Insert Removed from INOR-8 Pump Loop 9354-4. Etchant: 3 parts HCl, 2 parts H_2O, 1 part 10% chromic acid.

As previously reported,[1] a surface layer or film similar in appearance to that found on the 10,000-hr insert has been noticed on specimens removed from most of the long-time INOR-8 thermal- and forced-convection tests. Samples of this film are being studied, but no results are available. The band of precipitates and fine grains found along the surfaces of the inserts has not been observed in other tests of INOR-8. At present it is not known whether these fine grains represent a second phase or only recrystallization of the matrix near the inside surfaces of the insert. There is reason to suspect the latter possibility, since a reaming operation was performed on the inserts prior to service and undoubtedly induced some cold work along the inside surfaces. A review of the recrystallization properties of INOR-8 indicates that recrystallization of the material can be initiated at 1300°F following prior cold work.[2] Grain growth of the recrystallized material would be extremely slow at this temperature, which would help to explain the extremely fine crystallites apparent.

Examination of Three Inconel Pump Loops. – Chemical and metallographic results have been obtained for three Inconel pump loops which completed one year's operation. Operating conditions for these loops are shown in Table 2.1.2.

Metallographic examination of loop 9344-1, which circulated salt 123 for 8760 hr at a maximum temperature of 1300°F, showed heavy attack in the form of intergranular and general voids along both heater legs, as shown in Fig. 2.1.8. In the first heater leg, attack ranged from 18 to 31 mils in depth and in the second leg, from 18 to 38 mils.. The unheated bend

[2]J. Spruell, Recrystallization of INOR-8, ORNL CF-57-11-119 (Nov. 25, 1957).

Table 2.1.2. Operating Conditions for Three Inconel Forced-Convection Loops

Loop	Salt No.*	Maximum Salt-Metal Interface Temperature (°F)	Minimum Fluid Temperature (°F)	ΔT (°F)	Flow Rate (gpm)	Reynolds No.
9344-1	123	1300	1100	200	2	3250
9344-2	12	1200	1100	100	2.5	8200
9377-3	131	1300	1100	200	2	3400

*123: $NaF-BeF_2-UF_4$ (53-46-1 mole %)
12: NaF-LiF-KF (11.5-46.5-42 mole %)
131: $LiF-BeF_2-UF_4$ (60-36-4 mole %)

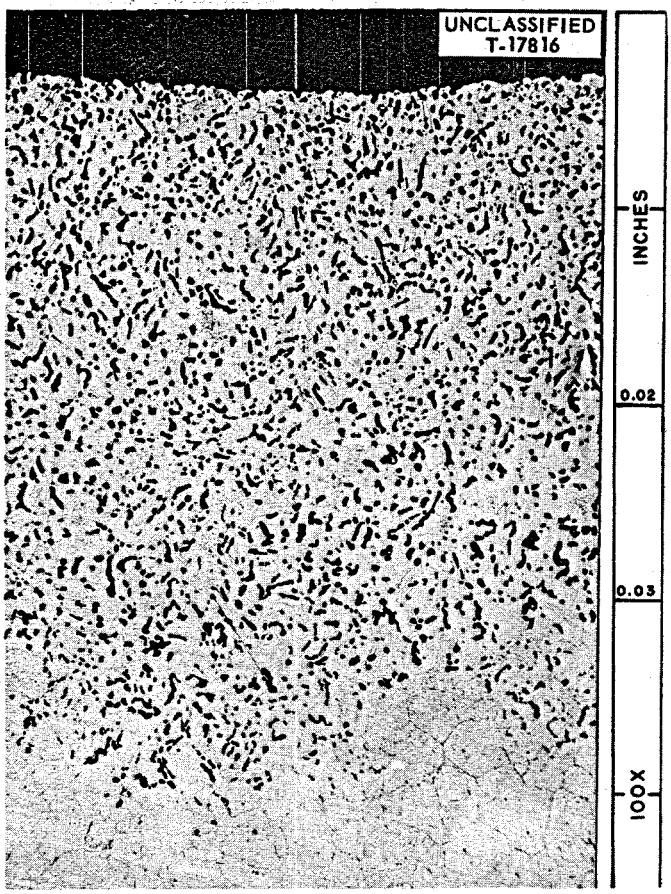

Fig. 2.1.8. Specimen Removed from End of Second Heater Leg of Inconel Pump Loop 9344-1, Showing Maximum Attack Found. Loop was operated for 8760 hr with salt mixture NaF-BeF_2-UF_4 (53-46-1 mole %). Etchant: modified aqua regia.

connecting the two legs revealed only a few pits, not over 1 mil, and the cold-leg sections showed only slight surface roughening and surface pitting. No cold-leg deposits were observed visually or metallographically.

Chemical analyses of the fused-salt mixture before and after circulation in this loop are shown in Table 2.1.3. Note that an extremely large increase in chromium concentration occurred during the test, along with a reduction in uranium concentration. Optical examination of the salt disclosed a brown phase consisting of about equal amounts of UO_2 and NaF-BeF_2. An x-ray examination of this phase confirmed the presence of UO_2. Thus the salt appears to have undergone extensive extraneous oxidation either before or during the test.

Metallographic examination of loop 9344-2, which operated for 8760 hr at a maximum temperature of 1200°F with salt 12, showed moderate attack in the form of intergranular and general voids along both heater legs. In

the first heater leg, attack ranged from 1 to 3 mils in depth and in the second leg, from 4 to 8 mils. The cold-leg sections and the unheated bend connecting the two hot legs revealed light intergranular voids to 1 mil. The coolant salt in this loop was replaced three times because of operating difficulties.

A somewhat higher rate of attack occurred in loop 9377-3, which circulated salt 131 for 8760 hr at a maximum temperature of 1300°F. Examination of the heater sections revealed attack in the form of heavy intergranular and general voids, ranging from 2 to 8 mils in the first heater leg and from 6 to 14 mils in the second leg. The unheated bend connecting the two legs showed only light surface roughening except in one region where a few isolated voids to a maximum depth of 11 mils were found. The cold-leg sections revealed only a few pits, all less than 1 mil.

Chemical analyses of salt 131 before and after circulation in loop 9377-3 are shown in Table 2.1.4. Except for the increase in chromium concentration, these analyses show little difference.

The present status of all forced-circulation loop tests now in progress is given in Sec 1.1 of this report.

Table 2.1.3. Analysis of Salt 123 Before and After Circulation in Pump Loop 9344-1

Sample Taken	Major Constituents (wt %)		Minor Constituents (ppm)		
	U	Be	Ni	Cr	Fe
Before test	3.40	8.16	140	425	130
After test	2.58	8.25	175	4670	205

Table 2.1.4. Analysis of Salt 131 Before and After Circulation in Pump Loop 9377-3

Sample Taken	Major Constituents (wt %)		Minor Constituents (ppm)		
	U	Be	Ni	Cr	Fe
Before test	19.6	7.12	145	345	200
After test	19.5	7.09	15	860	275

General Corrosion Studies

Permeation of Graphite by Molten Salts

The permeation of various grades of graphite by molten fluoride salts is being investigated in tests[3] at 1300°F (704°C) for 100 hr at 150 psig, using the weight increase of the test specimen to calculate the volume of graphite that is permeated by the salt. Table 2.1.5, a summary of results, lists 15 grades of graphite in order of resistance to permeation. These grades were manufactured as low-permeability graphite, with the exception of CT-158, CCN, CEYB, R-0013, AGOT, and TSF. The permeation values for the pipe material are considered high, because no effort was made to seal the ends of the pipe specimens to prevent the exposure of the more continuous and accessible voids produced in the axial direction as a result of fabrication. Pipe specimens with sealed ends are being made to be tested for permeation, since values for them should be more applicable to reactor designs.

Most of the testing was done with LiF-BeF_2-ThF_4-UF_4 (67-18.5-14-0.5 mole %); however, NaF-ZrF_4-UF_4 (56-40-4 mole %) and LiF-BeF_2-UF_4 (62-37-1 mole %) were also used. Under the test conditions the extent of permeation by the three salt mixtures was essentially the same; other test conditions will be investigated. No wetting of the graphite by the salts was observed.

Salt permeation studies with additional grades of graphite, including studies to show the effect of exposure time and graphite shape, were begun.

An effort is being made to preclude the fuel pickup by initially filling accessible void spaces in the graphite with bismuth, thus allowing no space for the salt. Approximately 60% of the accessible[4] void spaces of AGOT graphite specimens were filled with bismuth when held at 1022°F for 4 hr at 125 psig. Tests were begun to determine the extent to which these impregnated specimens will take up salt in standard permeation tests.

---

[3]W. H. Cook and D. H. Jansen, A Preliminary Summary of Studies of INOR-8, Inconel, Graphite, and Fluoride Systems for the MSRP for the Period May 1, 1958 to Dec. 31, 1958, ORNL CF-59-1-4, p 1–20.

[4]The total accessible void volume is reported to be 21.7% of the bulk volume of AGOT graphite; W. P. Eatherly, M. Janes, and R. L. Mansfield, "Physical Properties of Graphite Materials for Special Nuclear Applications," Second U.N. Intern. Conf. Peaceful Uses Atomic Energy, Geneva, 1958, paper A/Conf 15/P/708, p 4 (June 1958).

Table 2.1.5. Permeation of Various Grades of Graphite by Molten Fluoride Salts

All percentages are averages of three with the exception of those with numerical superscripts, which denote the number of values averaged

Graphite Grade	Graphite Bulk Density (g/cc)	Percentage of Bulk Volume of Graphite Permeated by Fluoride Salts[a]		
		Fuel 30	Fuel 130	BULT-14-.5U
GT-123-82	1.92			0.2
R-4	1.93			1.6
R-0009	1.92			1.8
CEY-82[b]	1.87			1.9
R-0009-RG	1.90			2.5
CT-158[c]	1.77			3.5
186	1.86		$4.6^{(1)}$	$3.8^{(6)}$
CCN	1.92	$4.9^{(1)}$	$4.2^{(2)}$	4.2
CEYB[b]	1.79			4.3
S-4	1.85			4.8
R-0013	1.87			6.0
ATJ-82-RG	1.83			6.4
CS-82-RG	1.80			8.1
AGOT	1.68	$14.8^{(1)}$	14.8	14.2
TSF	1.67		$13.2^{(2)}$	14.4

[a] 30: $NaF-ZrF_4-UF_4$ (56-40-4 mole %)
130: $LiF-BeF_2-UF_4$ (62-37-1 mole %)
BULT-14-.5U: $LiF-BeF_2-ThF_4-UF_4$ (67-18.5-14-0.5 mole %)

[b] Pipe, nominal dimensions, in.: 1-1/4 OD × 7/8 ID × 1/2 long.

[c] Pipe, nominal dimensions, in.: 25/64 OD × 3/16 ID × 1-1/2 long.

Removal of Oxide Contaminants from Graphite

Previous tests have shown that exposing graphite to fuel 130 ($LiF-BeF_2-UF_4$, 62-37-1 mole %) at 1300°F (704°C) will result in the precipitation of UO_2, and that this reaction is essentially complete within 5 hr when the fuel is in vapor-phase contact or in direct contact with the graphite. This indicated that oxide contamination might be removed from the graphite by vapor-phase or direct-contact gettering. Results that

indicated partial success in two such tests, with fuel 130 as the gettering agent, have been reported.[5]

A direct-gettering test, which has been completed, was apparently successful in removing oxide contaminants from the graphite. In the test a charge of fuel 130 was in direct contact with an AGOT graphite crucible for 20 hr at 1300°F (704°C) in a vacuum. The ratio of the bulk volume of the graphite to the volume of the salt was 27:1 (an arbitrary standard selected for such tests). Radiographic examinations at room temperature indicated that a normal quantity of UO_2 had precipitated. The gettering charge of fuel 130 was removed and replaced by a fresh charge of fuel 130, which was held an additional 20 hr at 1300°F. Radiographic examination showed no precipitation, indicating that the preceding gettering operation was successful.

Since the cost of fuel 130 would make it an uneconomical gettering agent to use on a full-scale reactor, cheaper gettering agents are also being investigated. A hydrogen test is in progress.

Tests similar to those described above are being made with LiF-BeF_2-ThF_4-UF_4 (67-18.5-14-0.5 mole %). Three such tests with AGOT graphite have continued for 500 hr, and no precipitation has been detected in the salt by radiographic examinations.

Compatibility of INOR-8 and Graphite in Direct Contact

The tendency for INOR-8 to carburize when in direct contact with graphite is being investigated as part of the over-all INOR-8–graphite–salt compatibility program. TSF-grade graphite and INOR-8 specimens were held in contact at 1300°F at 1000 psi. Modified stress-rupture apparatus was used, and the tests were held in salt environments to simulate reactor conditions. Metallographic examination of specimens held for 700 hr in NaF-KF-LiF-UF_4 (11.2-41-45.3-2.5 mole %) revealed no evidence of carburization. Tests for 3400 hr in NaF-ZrF_4-UF_4 (50-46-4 mole %) have been completed, and the test specimens are now being examined.

Brazing-Material Evaluation in Fuel 130

Since a barren-salt-to-fuel-salt heat exchanger is being considered for use in the Molten-Salt Reactor, the corrosion resistance of brazing

[5]MSR Quar. Prog. Rep. July 31, 1959, ORNL-2799, p 62.

alloys which may be useful in the fabrication of metal-to-metal joints in such a heat exchanger is being evaluated. The method used to subject brazing alloys to the corrosive environment in the hot leg of a thermal-convection loop has been described earlier,[6] and corrosion test results on a series of brazing alloys subjected to fuel 130 (LiF-BeF_2-UF_4, 62-37-1 mole %) for 1000 hr at a 1300°F hot-leg temperature in such a loop have been reported.[7]

The results of a 5000-hr test made under the same conditions are outlined in Table 2.1.6. Copper, gold-nickel, and the Coast Metals alloys showed good corrosion resistance. A depleted region to a depth of 3 mils was observed along each of the Coast Metals alloy fillets after the test. Results of earlier corrosion tests on these alloys in NaF-ZrF_4-base fuels and in liquid metals indicated that this depletion was due to the leaching of the minor constituents boron and silicon from the alloy by the bath, and it appears that boron and silicon are also being leached by fuel 130. This depletion has no detrimental effect on the alloy, since a nickel-rich, corrosion-resistant matrix is left. A 10,000-hr thermal-convection-loop test on Inconel and INOR-8 lap joints brazed with the five brazing materials listed in Table 2.1.6 is in progress.

Some refractory-metal-base alloys, being developed by the Welding and Brazing Group for possible application in joining graphite to graphite, were given a static corrosion test in fuel 130 for 100 hr at 1300°F. Nickel, because of its comparative inertness to fluorides, was used as the test-container material. Test results, listed in Table 2.1.7, showed large weight losses for each alloy. In order to determine the alloying element or elements responsible for the heavy attack, the following static corrosion tests in fuel 130 were conducted at 1300°F: (1) titanium was tested in containers of titanium, nickel, and INOR-8, (2) zirconium was tested in containers of zirconium, nickel, and INOR-8, and (3) beryllium was tested in a nickel container. Large weight losses (Table 2.1.8) were observed for specimens tested in nickel or nickel-base containers, while small weight losses were found when specimen and container were of the same metal. Substituting an INOR-8 (containing 70% Ni) container for one

[6]MSR Quar. Prog. Rep. June 30, 1958, ORNL-2551, p 62.

[7]Met. Ann. Prog. Rep. Sept. 1, 1959, ORNL-2839, p 166–67.

Table 2.1.6. Results of Metallographic Examinations of Brazing Materials Tested in Thermal-Convection Loop Circulating Fuel 130 (LiF-BeF_2-UF_4, 62-37-1 Mole %)

Test conditions: Hot-leg temperature, 1300°F
Cold-leg temperature, 1100°F
Time, 5000 hr

Alloy	Composition (%)	Metallographic Results: Alloy Brazed to	
		Inconel	INOR-8
Coast Metals No. 52	89 Ni–5 Si–4 B–2 Fe	No attack	No attack
Coast Metals No. 53	81 Ni–8 Cr–4 B–4 Si–3 Fe	No attack	No attack
General Electric No. 81	70 Ni–20 Cr–10 Si	Heavy attack of 16 mils	3-mil attack
Gold-nickel	82 Au–18 Ni	No attack	No attack
Copper	100 Cu	No attack; diffusion voids 2 mils deep on fillet	No attack; diffusion voids 2 mils deep

Table 2.1.7. Results of Static Corrosion Tests on Refractory-Metal-Base Brazing Alloys in Fuel 130 in Nickel Containers

Test conditions: 1300°F, 100 hr

Alloy Composition (%)	Weight Change (%)
48 Ti–48 Zr–4 Be	-4.2
95 Ti–5 Be	-6.5
95 Ti–5 Be	-9.8

Table 2.1.8. Results of Static Corrosion Tests on Refractory Metals in Fuel 130 in Containers of Several Materials

Test conditions: 1300°F, 100 hr

Material	Weight Change (%) When Tested in:			
	Nickel	INOR-8	Titanium	Zirconium
Ti	-12.1	-7.6	-0.71	
Zr	-11.7	-4.2		-0.08
Be	Excessive, portion of sample dissolved			

of pure nickel resulted in a weight-loss decrease on the titanium and zirconium specimens. Metallographic examination and spectrographic results on the nickel capsules revealed surface layers containing titanium, zirconium, or beryllium, corresponding to the major component of the brazing alloy or metal tested. Results of the tests indicate that the usefulness of titanium-, zirconium-, or beryllium-containing brazing alloys in fuel 130 would be limited in systems constructed of nickel or nickel-base alloys.

Phase Equilibrium Studies

The System BeF_2-ThF_4-UF_4

The most favorable fuels for breeding with molten fluorides are obtained from the LiF-BeF_2-ThF_4-UF_4 quaternary system. Of the ten binary and ternary systems which are incorporated as limiting cases in this quaternary system, only the system BeF_2-ThF_4-UF_4 has not been described previously. Spot checks have shown that only two primary phases, those of BeF_2 and of the ThF_4-UF_4 solid solution, are involved in the BeF_2-ThF_4-UF_4 phase diagram. As in the ThF_4-UF_4 binary system, no minimum exists in the ThF_4-UF_4 solid-solution liquidus surface in the ternary system. Isotherms for such of the liquidus surface in the ternary system can be approximated by straight lines between the bounding binary systems BeF_2-ThF_4 and BeF_2-UF_4.

The System BeF_2-ThF_4

Some of the information on previously reported[1] preliminary phase diagrams for BeF_2-ThF_4 was uncertain because BeF_2-ThF_4 mixtures containing more than 75 mole % BeF_2 are too viscous to reach equilibrium, even in periods as long as three weeks. This difficulty is greatly alleviated by small additions of NaF or LiF, and the BeF_2-ThF_4 binary diagram has now been established with the aid of short extrapolations from work on the ternary systems. Figure 2.2.1, showing a eutectic at 527°C and 2 mole % ThF_4, is regarded as a final diagram.

The System NaF-BeF_2-ThF_4

Continuing studies of the phase equilibria in the system NaF-BeF_2-ThF_4 have established that this system involves 12 invariant equilibrium points. Of these, ten have been established to within 1 mole % and 5°C; these ten are listed in Table 2.2.1.

Molten-Fluoride Solvents

A subsidiary interest, as far as breeder fuels are concerned, is attached to a recent search for alternate solvents for use in the fluoride-volatility dissolution process, in which a high solubility of ZrF_4 is a

---

[1] MSR Quar. Prog. Rep. Oct. 31, 1957, ORNL-2431, p 36.

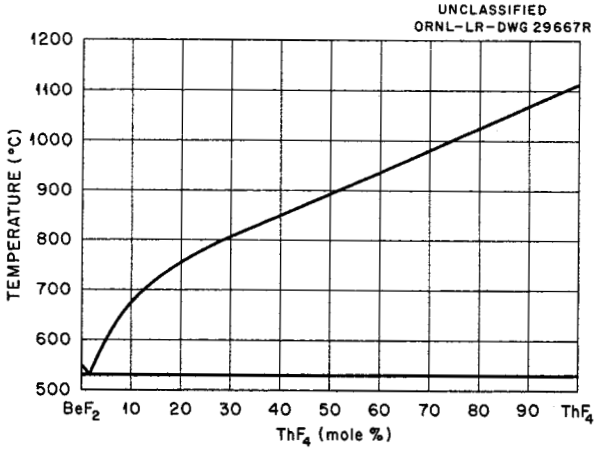

Fig. 2.2.1. The System BeF_2-ThF_4.

requisite. Three mixtures, NaF-ZrF_4, NaF-LiF, and NaF-LiF-ZrF_4, have been used; of these, NaF-LiF has the largest capacity for ZrF_4, but in this case liquidus temperatures approaching 600°C are encountered at 25 mole % ZrF_4.

Exploratory investigations of the phase equilibria in the system NaF-BeF_2-ZrF_4 have shown that NaF-BeF_2 (69-31 mole %) affords a solvent for ZrF_4 which will accommodate as much as 52 mole % of ZrF_4 in solution at temperatures below 550°C and that no liquidus temperatures higher than 570°C will be encountered on the composition path between NaF-BeF_2 (69-31 mole %) and NaF-BeF_2-ZrF_4 (33-15-52 mole %).

The Compound $NaF \cdot BeF_2 \cdot 3UF_4$

Studies by Barton et al.[2] on the system NaF-UF_4 and more recent attempts in this laboratory to synthesize a compound $NaF \cdot 4UF_4$ by thermal-gradient quenches of a substance with the composition 20 mole % NaF–80 mole % UF_4 have failed to confirm the existence of a compound with this composition, which was reported by Eichelberger et al.[3] in their investigation of the system NaF-BeF_2-UF_4. Moreover, studies at this laboratory in the system NaF-BeF_2-ThF_4 have shown that a primary-phase field exists corresponding to the "$NaF \cdot 4UF_4$" primary-phase field in the system NaF-BeF_2-UF_4 and that the primary phase in this case is $NaF \cdot BeF_2 \cdot 3ThF_4$. This compound is analogous in optical properties to the so-called "$NaF \cdot 4UF_4$" as

---

[2]C. J. Barton et al., J. Am. Ceram. Soc. 41(2), 63 (1958).

[3]J. F. Eichelberger et al., p 110 in Phase Diagrams of Nuclear Reactor Materials, R. E. Thoma, ed., ORNL-2548 (Nov. 6, 1959).

Table 2.2.1. Invariant Equilibria in the System $NaF-BeF_2-ThF_4$

Composition of Liquid (mole %)			Invariant Temperature (°C)	Type of Equilibrium	Solid Phases Present
NaF	BeF_2	ThF_4			
2	96	2	527	?	ThF_4, BeF_2, and $NaF \cdot BeF_2 \cdot 3ThF_4$
43	55	2	365	Eutectic	$NaF \cdot BeF_2$, BeF_2, and $NaF \cdot BeF_2 \cdot 3ThF_4$
49	49	2	375	?	$NaF \cdot BeF_2$, $NaF \cdot 2ThF_4$, and $NaF \cdot BeF_2 \cdot 3ThF_4$
47	51	2	375	Peritectic	$NaF \cdot BeF_2$, $NaF \cdot 2ThF_4$, and β-$NaF \cdot ThF_4$
56	42	2	320	Eutectic	$NaF \cdot BeF_2$, $2NaF \cdot BeF_2$, and β-$NaF \cdot ThF_4$
57	41	2	415	Peritectic	β_2-$2NaF \cdot ThF_4$, $2NaF \cdot BeF_2$, and β-$NaF \cdot ThF_4$
72	22	6	510	Eutectic	β_2-$2NaF \cdot ThF_4$, $2NaF \cdot BeF_2$, and NaF
76	11	13	540	Peritectic	β_2-$2NaF \cdot ThF_4$, β-$4NaF \cdot ThF_4$, and NaF
62	2	36	683	Peritectic	β_2-$2NaF \cdot ThF_4$, $3NaF \cdot 2ThF_4$, and β-$NaF \cdot ThF_4$
42	31	27	740	Peritectic	$NaF \cdot 2ThF_4$, ThF_4, and $NaF \cdot BeF_2 \cdot 3ThF_4$

reported by the Mound Laboratory. Since a thermal-gradient quench in the system $NaF-BeF_2-UF_4$ at 35-55-10 mole % has produced a primary phase which is isostructural, by x-ray diffraction analysis, with the compound $NaF \cdot BeF_2 \cdot 3ThF_4$, it seems probable that the compound reported by the Mound Laboratory is actually $NaF \cdot BeF_2 \cdot 3UF_4$.

Gas Solubilities in Molten Fluorides

Solubility of HF in Fuel Solvents

As previously reported,[4,5] the solubility of HF has been measured over wide composition ranges in both BeF_2- and ZrF_4-base solvents. In each type of system, compositions rich in alkali fluorides showed marked increases in the solubility and in the heat of solution of HF. The transition to higher values appeared to occur as the alkali fluoride content exceeded the stoichiometry for complete complexing of the Be^{++} as BeF_4^{--} and the Zr^{4+} as ZrF_7^{---}, thereby providing "free" fluorides for forming HF_2^-.

Several schemes were examined in an attempt to correlate the solubility of HF with the composition of the solvent. One which works well is the use of a composition scale in terms of equivalent per cent free NaF as shown in Fig. 2.2.2. Compositions corresponding to Na_2BeF_4 and Na_3ZrF_7 are considered to contain 0% excess NaF. Other compositions contain an excess or a deficiency of NaF; equivalents are calculated on the basis of 2 for Na_2BeF_4 and 3 for Na_3ZrF_7 in obtaining equivalent per cent compositions according to this scheme.

Figures 2.2.3, 2.2.4, and 2.2.5, applying to different temperatures, demonstrate the good correlation achieved for solubilities in $NaF-ZrF_4$ and $NaF-BeF_2$ compositions. Solubilities are expressed in terms of the Henry's law constant. The curves in the figures are logarithmic and give straight-line plots on semilog paper. The effects of both temperature and composition are accommodated in the expression

$$\log K = \left(\frac{8400 + 3263\ RC}{RT} - \frac{15.24 + 0.909\ RC}{R} \right) ,$$

---

[4] MSR Quar. Prog. Rep. Oct. 31, 1958, ORNL-2626, p 85.

[5] MSR Quar. Prog. Rep. Jan. 31, 1958, ORNL-2474, p 93.

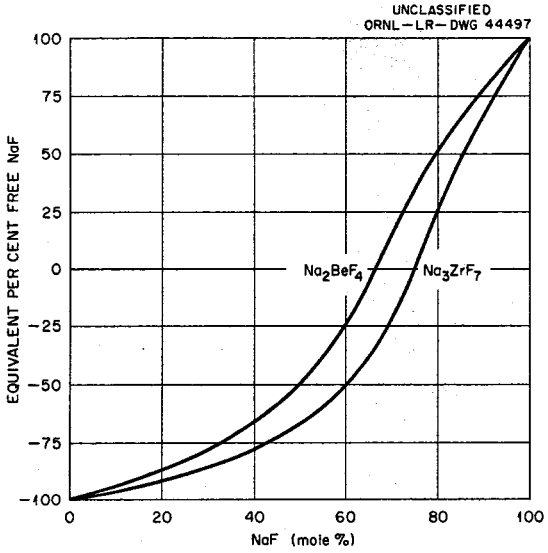

Fig. 2.2.2. Correlation of Free NaF with Mole Fraction of NaF in Mixtures of NaF-BeF_2 and NaF-ZrF_4 (Based on Na_2BeF_4 and Na_3ZrF_7).

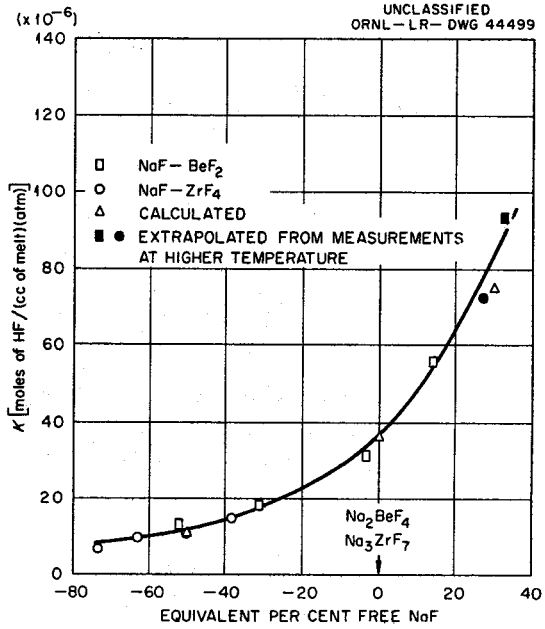

Fig. 2.2.4. Composition Dependence of Henry's Law Constants for the Solubility of HF in NaF-BeF_2 and NaF-ZrF_4 Mixtures at 700°C.

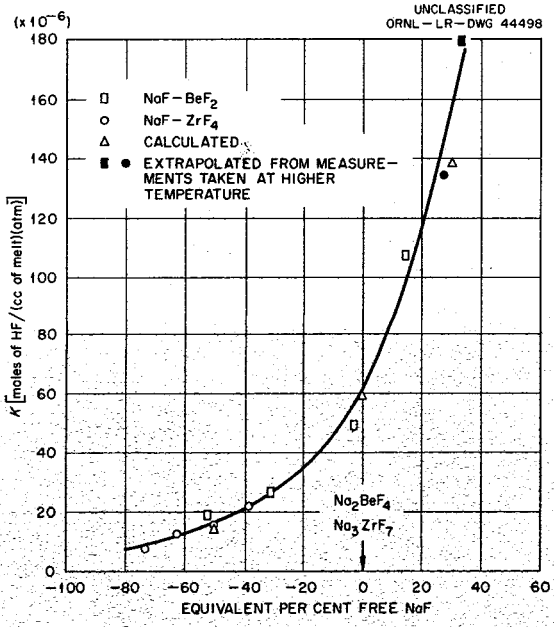

Fig. 2.2.3. Composition Dependence of Henry's Law Constants for the Solubility of HF in NaF-BeF_2 and NaF-ZrF_4 Mixtures at 600°C.

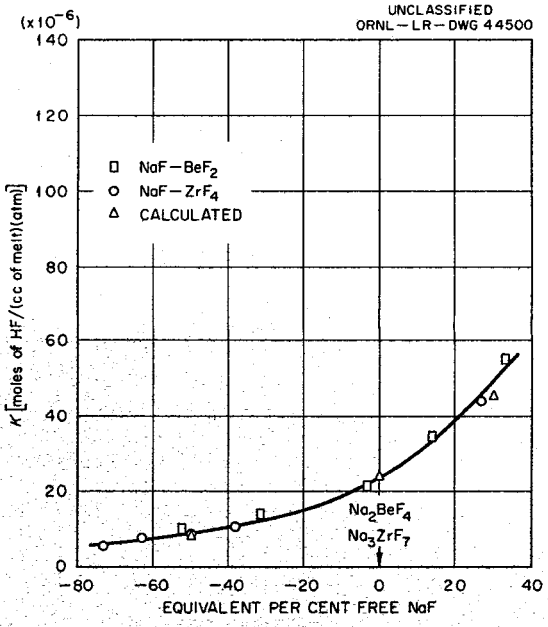

Fig. 2.2.5. Composition Dependence of Henry's Law Constants for the Solubility of HF in NaF-BeF_2 and NaF-ZrF_4 Mixtures at 800°C.

where

K = Henry's law constant, moles of HF/(liter of melt) (atm),

C = concentration of effective free fluoride, equivalent per cent,

T = temperature, °K,

R = gas constant.

Calculated values from this equation, denoted by triangles in Figs. 2.2.3 to 2.2.5, are within the experimental precision of the measurements.

The arbitrary concentration scale used here can be related to a more conventional concentration concept by considering the system NaF-BeF_2 to be composed of the systems BeF_2-Na_2BeF_4 and Na_2BeF_4-NaF; then the postulated free-fluoride model corresponds to mole % BeF_2 in the former system and to equivalent per cent NaF in the latter system. Similar relations hold for the NaF-ZrF_4 system.

Fission-Product Behavior

Exchange Reactions in Molten Fluorides

Experiments with exchange reactions for reprocessing molten-salt reactor fuels have continued.[6] Important characteristics for potential solid exchange reactants are insolubility in molten fluorides and chemical inertness toward reactor fuel constituents.

Studies of oxide reactions in molten fluorides have shown that the rare-earth oxides are sufficiently insoluble to qualify as possible exchange agents. The exchange of CeO_2 with cerium ion in the solvent LiF-NaF (60-40 mole %) and the effect of subsequently added CeF_3 on the equilibrium

$$Ce^*F_3(\ell) + CeO_2(s) \rightleftharpoons Ce^*O_2 + CeF_3$$

are shown in Fig. 2.2.6. Similarly, in the same solvent, the removal of lanthanum-tracer activity with La_2O_3 and the effect of subsequent additions of CeF_3 are shown in Fig. 2.2.7. These experiments, while not carried out in realistic fuels, nevertheless illustrate the effectiveness of exchange processes in molten fluorides. The exchange of lanthanum with cerium is interesting as a possible method for replacing nuclear poisons, such as samarium, gadolinium, and europium, with more innocuous rare earths such as cerium. Unfortunately, as shown in Fig. 2.2.8, CeO_2 reacts readily with

[6] MSR Quar. Prog. Rep. July 31, 1959, ORNL-2799, p 81.

UF_4 in the solvent LiF-NaF (60-40 mole %). Hence, reprocessing with rare-earth oxides would probably be limited to reactor fuels from which uranium had been removed by prior treatment. Figure 2.2.9 illustrates the unfavorable effect of ThF_4 and BeF_2 on the removal of tracer-cerium activity from solution by exchange with CeO_2.

Experiments to investigate the exchange properties of carbides are also under way. The results of two experiments to study the removal of hafnium activity with hafnium carbide are shown in Fig. 2.2.10. These results illustrate the unfavorable effect of UF_4 on the exchange reaction in the solvent LiF-BeF_2 (63-37 mole %).

Attempts to remove barium activity with Cr_2O_3 and BeO from the solvent LiF-BeF_2-ThF_4 (67-18-15 mole %) were not successful. Similarly an attempt to remove cerium activity from the same solvent with BeO was unsuccessful. The addition of Al_2O_3 to LiF-BeF_2-ThF_4 (67-18-15 mole %) containing cerium activity caused the precipitation of ThF_4 without any detectable removal of cerium activity from solution.

These experiments show that exchange reactions for reprocessing molten-salt reactor fuels are in many cases adversely affected by essential constituents in the fuels. The presence of thorium and beryllium, for example, interferes with exchange reactions involving CeO_2 and HfC. Further searches for suitable exchange agents will include the rare-earth carbides.

Chemistry of Corrosion Processes

Self-Diffusion Coefficients for Chromium in Nickel Alloys

A preponderance of the evidence accumulated over many years indicates that corrosion of nickel-chromium alloys by molten fluorides under anisothermal conditions should reach a steady-state rate controlled by diffusion of chromium in the metal in the colder part of the system. For this reason the value of the diffusion coefficient for chromium has been of paramount interest.[7]

Data from several diffusion experiments, employing Cr^{51} as a tracer, have been partially digested. The alloy specimens studied may be grouped as follows, according to the treatment they received prior to the experiments: Inconel annealed at 800°C for 8 to 12 hr, Inconel annealed at

[7]MSR Quar. Prog. Rep. Oct. 31, 1958, ORNL-2626, p 99.

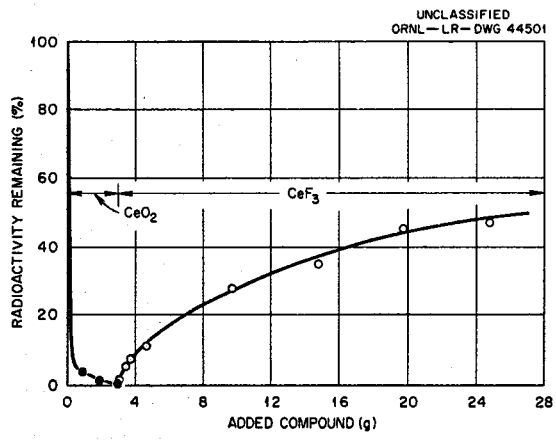

Fig. 2.2.6. Exchange of Cerium Activity with CeO_2 and CeF_3 in LiF-NaF (60-40 Mole %) at 750°C.

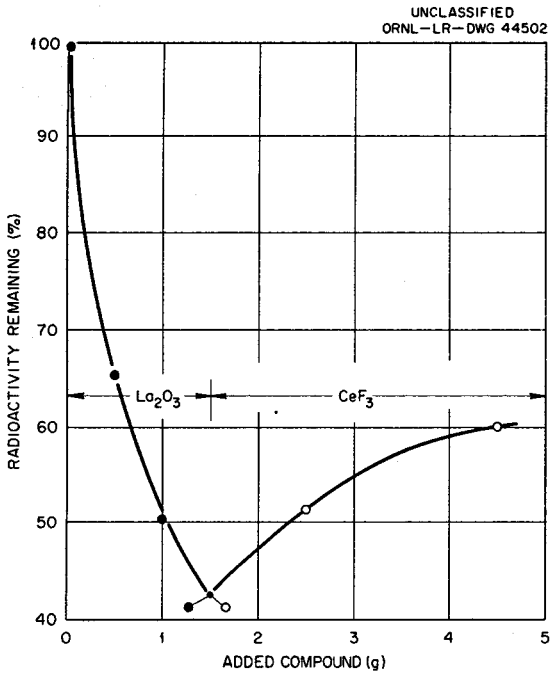

Fig. 2.2.7. Exchange of Tracer-Lanthanum Activity with La_2O_3 and CeF_3 in LiF-NaF (60-40 Mole %) at 750°C.

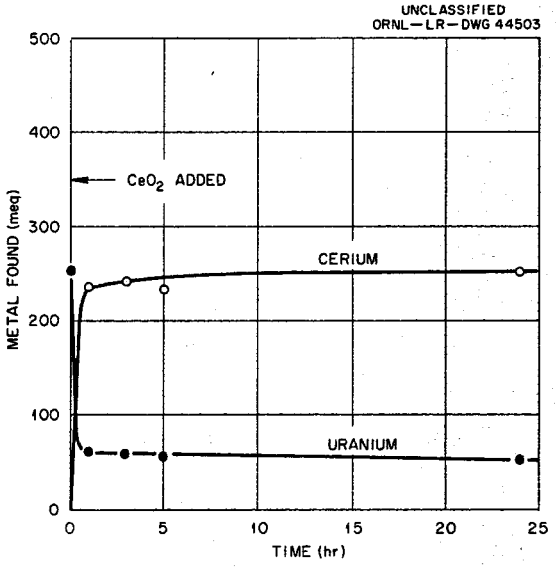

Fig. 2.2.8. Reaction of UF_4 with CeO_2 in LiF-NaF (60-40 Mole %) at 750°C.

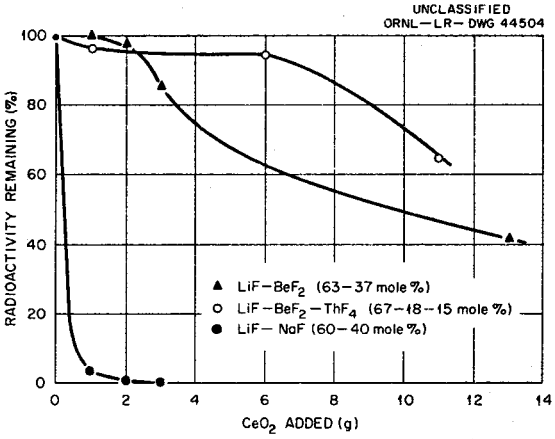

Fig. 2.2.9. Removal of Tracer-Cerium Activity by Exchange with CeO_2 in Molten Fluoride Systems.

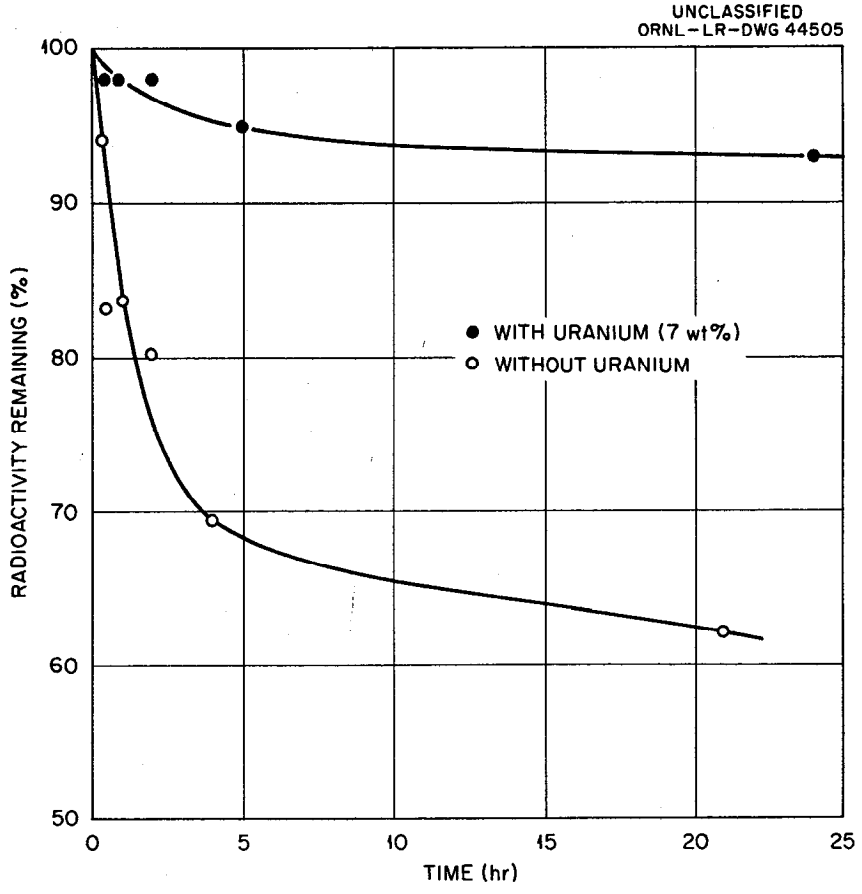

Fig. 2.2.10. Effect of UF_4 on the Removal of Hf^{181} Activity with HfC (5 wt %) in LiF-BeF_2 (63-37 Mole %) at 600°C.

1150°C for 2 to 4 hr, and INOR-8 annealed at 800°C for 8 to 12 hr. The results given here are over-all coefficients obtained from a comparison between the total amount of Cr^{51} present in the metal and the amount in the contacting salt after a given exposure time. A description of the experimental procedures was given in previous reports.[7,8] The data presently under discussion are not based on concentration profiles within the alloy. Companion experiments of the latter type will be discussed in a subsequent report; the general trends discussed below are reflected by the available profile data.

The results for Inconel specimens are presented as curves 5 and 7 on Fig. 2.2.11. Only two experimental points for Inconel specimens are shown; however, curve 5 was taken from 19 individual points (34 experiments) at various temperatures, and curve 7 from 16 points. Curves 1 through 4, from

[8]MSR Quar. Prog. Rep. June 30, 1958, ORNL-2551, p 95.

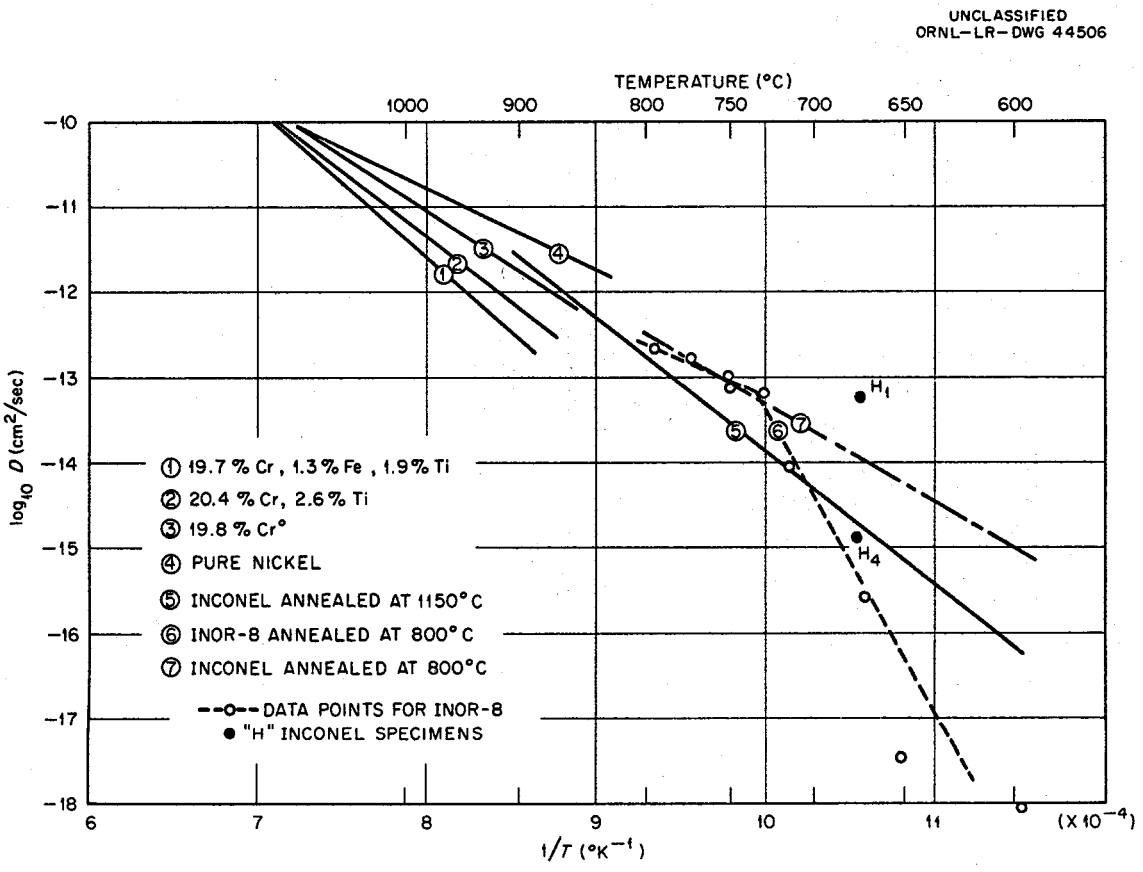

Fig. 2.2.11. Diffusion Coefficients of Cr^{51} in Various Nickel-Base Alloys.

a high-temperature investigation conducted on similar alloys by Russian investigators,[9] are shown for comparison.

It has been found that grain size, and therefore the annealing history prior to the diffusion experiments, has a marked effect on the diffusion coefficients. For example, photomicrographs of Inconel specimens H_1 and H_4 revealed that the average grain size was much greater in H_4 than in H_1. The effect of annealing conditions is easily seen by comparing curves 5 and 7 of Fig. 2.2.11 and also the individual values for H_1 and H_4. An additional annealing effect is manifest in the reproducibility of diffusion behavior. The data of curve 7 (specimens annealed at 800°C) tend to show a higher degree of scattering than those of curve 5 (specimens annealed at 1150°C), which suggests that an 800°C annealing temperature fails to eliminate grain variations which might exist between specimens.

[9]P. L. Gruzin and G. B. Fedorov, Doklady Akad. Nauk S.S.S.R. 105, 264 (1955).

The over-all diffusion coefficients obtained for INOR-8 specimens are shown as points on curve 6 of Fig. 2.2.11. At temperatures greater than 700°C, the INOR-8 coefficients are of the same magnitude as the Inconel coefficients. This means that the rates of chromium diffusion in INOR-8 are approximately 7/15 of the rates in Inconel, at least at higher temperatures. The ratio 7/15 corresponds to the ratio of the chromium concentrations in the alloys.

At temperatures below 700°C, the INOR-8 coefficients appear to fall considerably below the Inconel coefficients. This sudden drop might afford a partial explanation of the encouragingly low molten-salt corrosion rates exhibited by INOR-8 within the 500 to 700°C temperature range.

Another point of interest is that observed corrosion results frequently represent considerably faster rates than predicted on the basis of diffusion in the cold zone as the rate-controlling step if the diffusion coefficients from Fig. 2.2.11 are used. This suggests that there is frequently an extended period of uncompensated oxidation, largely extraneous, which precedes the establishment of a steady-state regime. An extreme example of this is described in the next section.

Chemical Analyses of Corrosion Test Loops

Periodic sampling to follow the corrosion behavior in pumped loop systems has continued.[10] An INOR-8 loop, containing $LiF-BeF_2-ThF_4-UF_4$ (62-36.5-1-0.5 mole %) has been operating for 9300 hr with a hot-zone temperature of 1300°F and a cold-zone temperature of 1100°F. As shown in Fig. 2.2.12, the chromium content reached a steady-state value of 500 ppm after about 1000 hr. Sampling was temporarily discontinued after 5000 hr in order to maintain a sufficient fuel volume in the loop; the scheduled test period for the loop is 15,000 hr. This loop appears to be following the predicted behavior.

By contrast, an Inconel loop, operating under the same conditions, has shown a steady increase in chromium concentration in the fuel as illustrated in Fig. 2.2.13. After about 2000 hr some additional fuel was added to compensate for the depletion due to sample removals. A slight dilution of the chromium ion concentration was reflected in the analyses. At about 3000 hr a motor failure necessitated draining the loop into the

[10] MSR Quar. Prog. Rep. July 31, 1959, ORNL-2799, p 88.

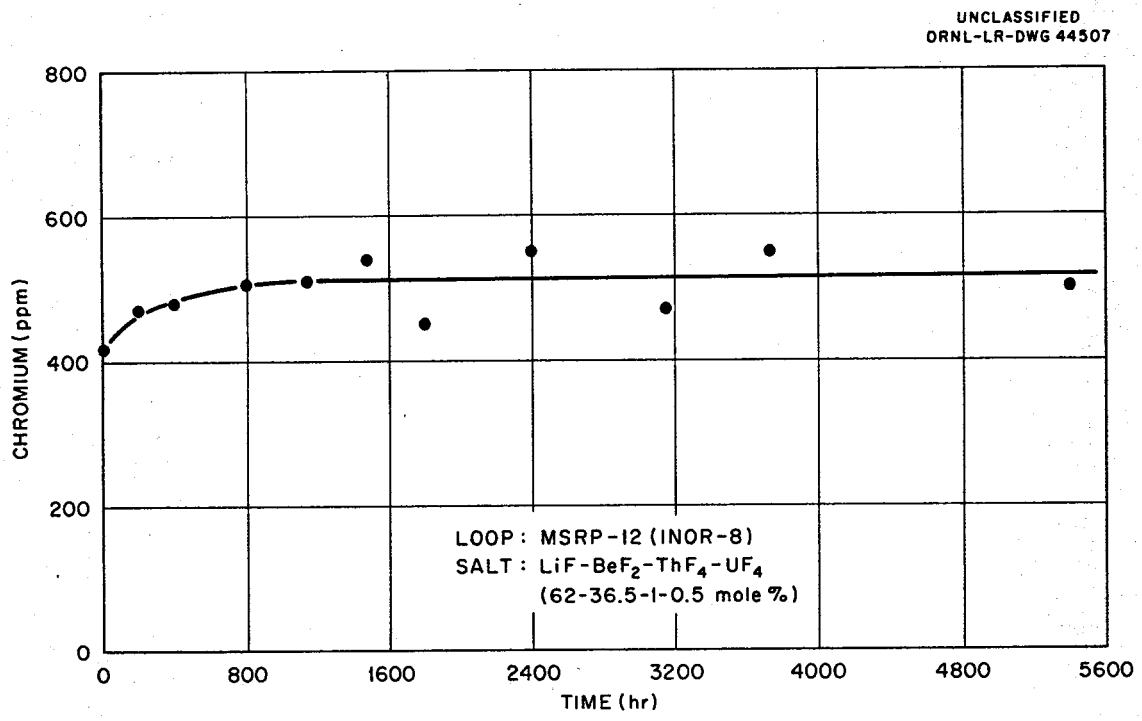

Fig. 2.2.12. Chromium Concentration Due to Corrosion of INOR-8.

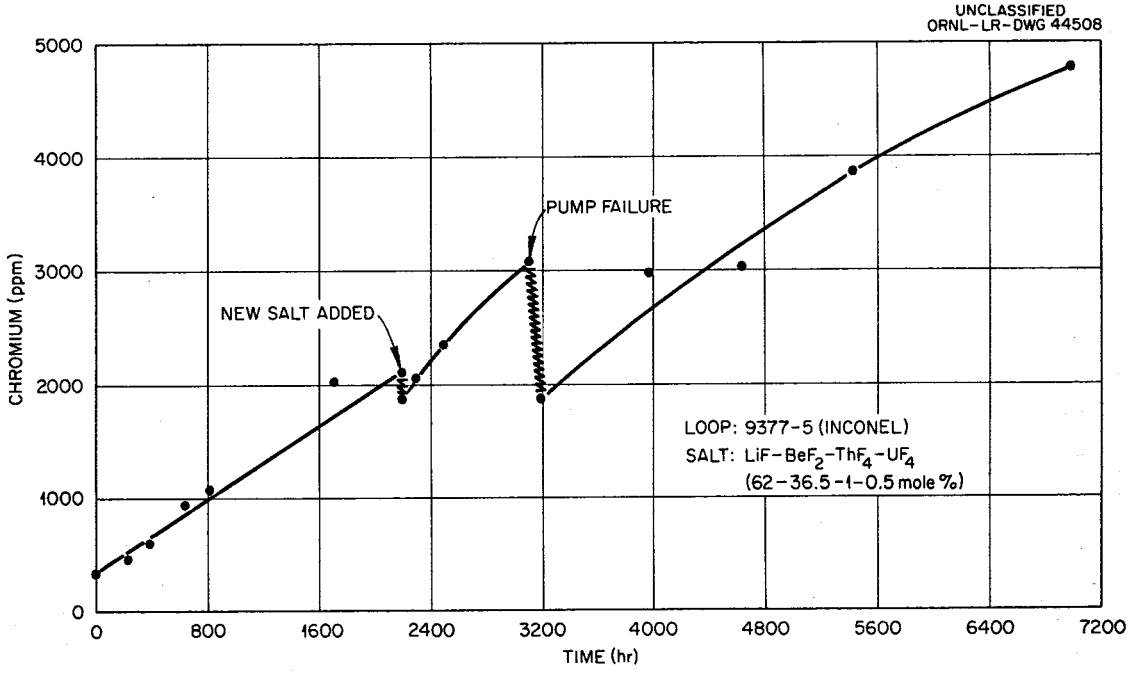

Fig. 2.2.13. Corrosion of Inconel Due to an Unidentified Extraneous Source.

sump; this resulted in another dilution because, contrary to intended operating procedures, a large residue of uncirculated salt had remained in the sump since the original filling. As the chromium concentration has increased to 4730 ppm in 7000 hr, the uranium concentration has dropped from 2.8 to 1.5 wt %. This is the behavior predicted for continuing exposure to an extraneous oxidant, such as air, but a rigorous examination of the system did not disclose any evidence of a leak or other means of exposure to air.

In another loop, of INOR-8, a salt mixture with a higher concentration of uranium, $LiF-BeF_2-UF_4$ (70-10-20 mole %), has been pumped under similar conditions for 5500 hr. The analyses suggest, as shown in Fig. 2.2.14, that the expected steady-state chromium concentration has not yet been reached; this is somewhat surprising.

Three additional test loops, scheduled for periodic sampling, were placed in operation during the past quarter.

Solubility of CrF_2 in $LiF-BeF_2$ (62-38 Mole %)

The solubility of CrF_2 in $LiF-BeF_2$ (62-38 mole %) was found to be greater than 7.0 mole % at 483°C. Uncombined CrF_2 was found to be precipitated from the melt, containing 7.0 mole % CrF_2, at 369 to 422°C at the phase boundary between CrF_2 and $2LiF \cdot BeF_2$ primary-phase fields.

Besides indicating the extremely high concentration of CrF_2 required for deposition on heat exchanger surfaces, this information should lead

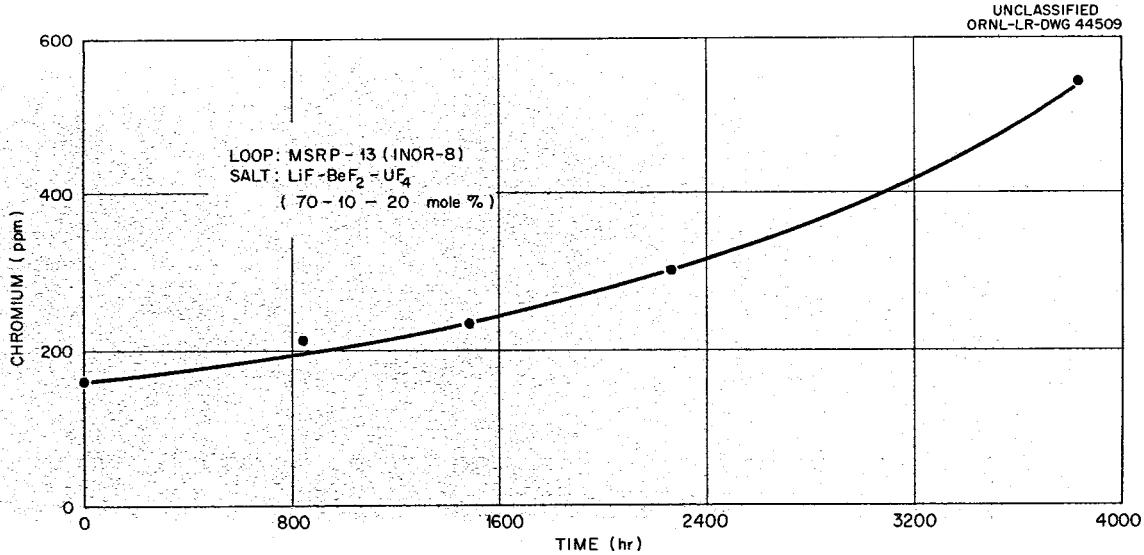

Fig. 2.2.14. Corrosion of INOR-8 by Fuel Containing a High Concentration of UF_4.

to an experimental determination of the free energy of formation for pure CrF_2 at high temperatures (800°C) when combined with the equilibrium constants now being obtained for the reaction

$$CrF_2 + H_2 \rightleftharpoons Cr^0 + 2HF$$

Equilibrium Measurements on the Reduction of CrF_2 and FeF_2 by H_2 in LiF-BeF_2 (62-38 Mole %)

High-temperature experimental equilibrium quotients,[11] K_x, for the reduction of CrF_2 and FeF_2 dissolved in LiF-BeF_2 (62-38 mole %) are being obtained from the following reactions:

$$CrF_2 + H_2 \overset{800°C}{\rightleftharpoons} Cr^0 + 2HF$$

$$FeF_2 + H_2 \overset{700°C}{\rightleftharpoons} Fe^0 + 2HF$$

A comparison of recent experimental equilibrium quotients obtained for the above reactions with those for the same reactions in NaF-ZrF_4 (53-47 mole %) is shown in Table 2.2.2.

The saturating phase for CrF_2 in LiF-BeF_2 (62-38 mole %) is pure CrF_2; a complex compound precipitated on saturating NaF-ZrF_4 (53-47 mole %) with

[11] MSR Quar. Prog. Rep. July 31, 1959, ORNL-2799, p 85.

Table 2.2.2. Effect of Solvent on the Equilibrium Quotients (Atmospheres/Mole Fraction), $K_x = M^0 P^2_{HF} / X_{MF_2} P_{H_2}$

Compound	Temperature (°C)	K_x	
		In LiF-BeF_2	In NaF-ZrF_4[a]
		$\times 10^{-4}$	$\times 10^{-4}$
FeF_2	700	~4500[b]	6300
CrF_2	750	1.8[c]	2.21
	800	4.1[c]	6.77

[a] ANP Quar. Prog. Rep. Mar. 10, 1956, ORNL-2061, p 84.

[b] 2.88 mole % FeF_2.

[c] 0.53 mole % CrF_2.

CrF_2 or FeF_2. Previous studies have indicated that the saturating phase for FeF_2 in LiF-BeF_2 (62-38 mole %) is pure FeF_2; this is still being verified. The smaller equilibrium quotients in LiF-BeF_2 result from stronger complexing in a more basic solvent.

Hygroscopic Behavior and Dehydration of Breeder Fuels

It has been generally recognized that breeder fuels based on LiF-BeF_2 as solvent are very hygroscopic and prone to hydrolysis, but no specific experimental evaluation of the problem had been made. Some salts can be dried without extensive hydrolysis, and drying at low temperatures is frequently helpful.[12] Trials were made to explore the prospects for removing water from breeder fuels at low temperatures. Two compositions, LiF-BeF_2-UF_4 (62-37-1 mole %) and LiF-BeF_2-ThF_4-UF_4 (62-36.5-1-0.5 mole %), were prepared by melting with ammonium bifluoride. These preparations were then examined by x-ray diffraction and microscopic techniques and found to be typical samples. Only traces of UO_2 were present.

A sample of each, ground to 100 mesh and weighing approximately 10 g, was placed in a nickel crucible and exposed to water-saturated air at room temperature. The initial rate of weight increase was 2.0% per day for each composition. As exemplified in Fig. 2.2.15, for the sample with ThF_4, after 40 days the total weight of the sample had increased by 23% and the rate of increase was 0.32% per day; for the sample without ThF_4 the corresponding values were 30% and 0.38% per day. These weight percentages are based on the original weight before exposure. The samples were then placed in an oven exposed to air at 133°C. Within 24 hr they had returned to the original weights. But on continuing the drying to obtain a constant weight, the samples continued to drop very slowly to values 0.3 and 0.4%, respectively, below the starting weight. Unfortunately, the salts at this state could not be distinguished from uncontaminated fuel by either x-ray diffraction or petrographic techniques.

The samples were then melted in a vacuum dry box at 30 to 50 μ, and a release of gas bubbles was observed. There was a further weight loss of 0.6 and 1%, respectively, for the samples with and without ThF_4. At this stage the samples were predominantly green with many small black

[12]Argonne National Laboratory, Reactor Fuel Processing 2(4), 42 (1959).

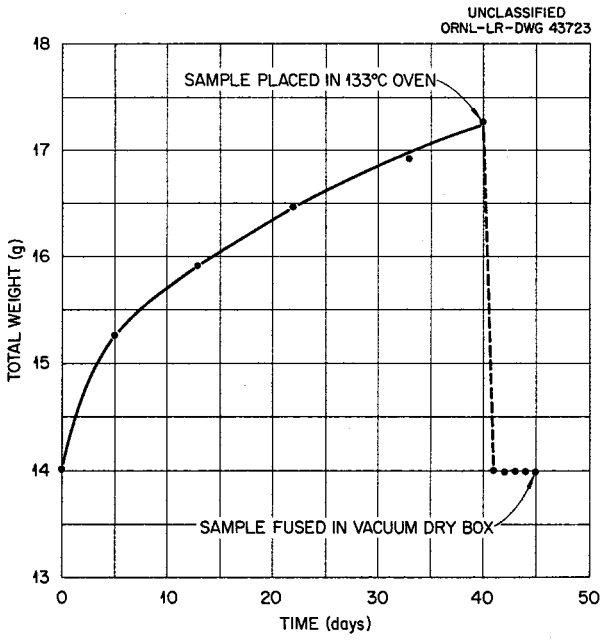

Fig. 2.2.15. Hydration-Dehydration Cycle for $LiF-BeF_2-ThF_4-UF_4$ (62-36.5-1-0.5 Mole %).

areas. The green portion had a higher UO_2 content than the starting materials; the black portions were predominantly UO_2, and it was estimated that from 20 to 40% of the uranium had been converted to UO_2. Evidently the uranium had served as an oxide scavenger for the melt.

A second pair of samples was treated as above except that the baking in air was eliminated. Each sample went directly from the humidifier to the vacuum dry box, where it was dried at 135°C for 2 hr at 30 to 50 μ and then melted. Bubbling occurred as before, and the final samples were 1.5 and 1% below the starting weight. The samples fused after vacuum drying were essentially identical with the fused samples from the first experiment.

It was concluded that the weight losses on prolonged drying were at least in part due to the substitution of O (wt 16) for 2F (wt 38) as a consequence of hydrolysis, and that a satisfactory reconditioning of fuel by a simple drying operation is unlikely.

Graphite Compatibility Studies

Penetration of Graphite by Molten Fluorides

Continuing studies[13] of the permeation of graphite by fuel mixtures at approximately 1 atm led to the following conclusions.

Early experiments, in which only slight permeation of graphites such as AGOT occurred, reflected the effect of surface oxide in the graphite as a source of plugging by the formation of insoluble UO_2. Such results could be altered to give easy permeation by using fuels with a larger oxide solubility, or by previously removing the oxide by treatment with H_2. When easy permeation was achieved, the relative composition of the fuel in the graphite was normal, in contrast to the earlier behavior which involved complications due to oxide precipitation. Long-term tests gave the same amount of permeation as short ones. There was good agreement between the permeation obtained by experiment, in the absence of oxide interference, and the permeation calculated on the basis of the physical interaction between a nonwetting liquid and a porous medium.

Tests at lower pressures have been discontinued in favor of more pertinent studies at 60 psig, corresponding to reactor conditions. At these higher pressures the permeation is increased in the expected manner, and differences in behavior due to the presence of oxide are usually not apparent. For example, when dealing with a readily permeable graphite, such as AGOT, little effect is noted as a result of pretreatment with H_2.

Attention has recently centered on the amount of permeation to be expected at 60 psig in various grades of graphite; typical results are shown in Table 2.2.3. In the usual procedure the graphite specimens were baked out under 40-μ partial vacuum at 1300°F for 24 hr and then left in contact with the salt at 60 psig and 1300°F.

A test of graphite coated with siliconized silicon carbide was accidentally invalidated when, as later realized, the coating was punctured during mounting for submersion in molten fuel. Consequently, ensuing large weight gains were not necessarily attributable to failure of the coating. From a metallurgical examination it appeared that the coating had been severely attacked, but no definite conclusions could be reached because no specimens in the original condition were available for comparison.

---

[13] MSR Quar. Prog. Rep. July 31, 1959, ORNL-2799, p 90.

Table 2.2.3. Permeability of Various Graphites

Permeation conditions: temperature, 1300°F; pressure, 60 psig

Graphite	Weight Gains (%)	
	$LiF-BeF_2-ThF_4$ (67-18-15 mole %)	$LiF-BeF_2-ThF_4-UF_4$ (67.0-18.5-14.0-0.5 mole %)
AGOT	17–22	20–23
TSF	19	
R-0013	10	
S-4	4.6–7.0	3.6
21-CT-158	-0.1	-0.1
18-CT-158	-0.1	-0.1
GT-123	±0.1	±0.1
ATL-82	6.2	
CEY* (RLM-24)	Not completed	0.1–0.2
CEY** special	1.0	Not completed

*Extruded tubing, 1-1/4-in. OD × 7/8-in. ID.
**Extruded tubing, 1/2-in. OD.

Intercalation of Graphite with Molten Salts

The possibility of intercalation compounds of graphite and molten fluorides is unlikely, in view of the wide experience in handling fuels in graphite with no evidence of chemical reaction. However, because of the prevalence of intercalation of chloride with graphite,[14] it was of interest to explore the phenomenon.

Of the 20 principal fission elements, niobium, technetium, and possibly molybdenum fluorides seemed most likely to exhibit intercalation with graphite. Most of the other fission-element cations form stable fluorides which have been included in melts in graphite crucibles in the course of other investigations in the Reactor Chemistry Division. Also, the more noble metals would be expected to exist as the free element and therefore would not intercalate. While molybdenum is also likely to be uncombined, it could possibly form a low-valence fluoride. Fluorides of molybdenum with a valence lower than six have been studied very little. Niobium forms

[14]W. Rüdorff, "Graphite Intercalation Compounds," in Advances in Inorganic Chemistry and Radiochemistry, H. J. Emelens and A. G. Sharpe, eds., p 223–266, vol. I, Academic Press, New York, 1959.

a stable pentafluoride which has not yet been evaluated in graphite. Very little is known of the chemistry of technetium, but it seems to resemble rhenium more closely than it does manganese.

When treated with molten molybdenum pentafluoride, graphite swelled to form an intercalate. A graphite tube (3/8-in. OD, 1/4-in. ID) was sealed in a copper capsule with MoF_5 and maintained at 100 to 150°C for 17 hr. The unreacted MoF_5 was distilled off by heating to 200°C. As a result of the treatment part of the graphite tube had crumbled, but the outside diameter of the intact portion had increased to 1/2 in. Exposure to water caused the tube to evolve heat and hydrogen fluoride in a manner similar to the behavior of pure MoF_5.

Molybdenum hexafluoride also gave evidence of intercalation, and a similar phenomenon has been noted repeatedly with UF_6. Such strong oxidizing agents as these could not survive in a reactor, but would be reduced to a lower valence state by reaction with the containing walls.

Diffusion of Rare-Earth Fission Products in Graphite

The development of techniques for the study of diffusion of rare earths in graphite is in progress. Specimens of graphite are to be impregnated with breeder fuels containing a trace quantity of $Eu^{152,154}$. The activity distribution in the graphite will be determined before and after exposure to clean fuel salt by microcore drilling of small graphite samples from the face of a section of the graphite rod. Tube furnaces, furnace controllers, and Inconel fuel containers for the leaching operation have been procured. Equipment for microcore drilling has been designed and fabricated and the technique tested on graphite samples containing Cs^{137}. This technique will be adapted for use in the hot cell to analyze graphite samples from the MTR graphite–fused-salt experiment. A simple glove box for contamination control is under construction, and a saw for sectioning the graphite rod is on order. Specimens of graphite for the first test were received, were machined to the desired dimensions, and are ready for impregnation.

Preparation of Purified Materials

Technological Operations

In order to stock-pile sufficient quantities of fluoride salt mixtures to supply the Molten Salt Reactor Program for the remainder of this

fiscal year, the production facility was activated for three weeks, and 600 kg of fluoride salt mixes was processed. Small-scale processing operations accounted for another 140 kg, making a total of 740 kg.

The increased rate of transfer and service operations encountered during the previous quarter continued during the first month of this quarter; the rate then dropped. Considerable effort has been devoted to developing a technique for filling recently designed in-pile capsules[15] for testing graphite. The results obtained to date are promising but not completely satisfactory.

Molten Ammonium Bifluoride as a Reagent

Reactions of molten ammonium bifluoride have been useful for preparing a large number of metal fluorides and ammonium fluometallates.[16] Additional reactions of ammonium bifluoride have been explored.

Ammonium dichromate dissolved in ammonium bifluoride at 125°C to form an orange melt which vigorously bubbled and rapidly became green at about 200°C. Ammonium hexafluochromate(III) had formed by the following reaction:

$$6NH_4HF_2 + (NH_4)_2Cr_2O_7 \rightarrow 2(NH_4)_3CrF_6 + 7H_2O\uparrow + N_2\uparrow$$

Chromic acid reacted similarly:

$$8NH_4HF_2 + 2CrO_3 \rightarrow 2(NH_4)_3CrF_6 + 6H_2O\uparrow + N_2\uparrow + 4HF\uparrow$$

Cerium trifluoride was prepared by the thermal decomposition of a complex, presumably ammonium hexafluocerate(III), made by reacting molten ammonium bifluoride with ceric oxide:

$$20NH_4HF_2 + 6CeO_2 \xrightarrow{200°C} 12H_2O\uparrow + 4HF\uparrow + N_2\uparrow + 6(NH_4)_3CeF_6$$

$$(NH_4)_3CeF_6 \xrightarrow{600°C} CeF_3 + 3NH_3\uparrow + 3HF\uparrow$$

Lithium hydroxide monohydrate, enriched in isotope 7, was converted into the anhydrous fluoride by fusion with ammonium bifluoride and eliminating volatiles at about 350°C.

---

[15]For the ORNL-MTR-47 experiment.

[16]MSR Quar. Prog. Rep. Apr. 30, 1959, ORNL-2723, p 93–94.

Radiation Effects

Corrosion Tests Under Radiation

Two static-corrosion capsules, made of INOR-8 alloy, were irradiated in the Materials Testing Reactor. Fuel composition and test conditions are summarized in Table 2.2.4.

Failure became evident from the release of radioactivity into the off-gas from one of the capsules. The two capsules were installed as a unit; so it was necessary to terminate the test for both capsules.

The Chromel-Alumel thermocouples attached to the capsules showed no sign of failure, and the capsules are being removed from the reactor by a process designed to preserve the thermocouples. The capsules will be examined in the hot cells at ORNL.

Metallographic tests will be made on the metal, chemical analyses will be made on the fuel, and calibrations will be made on the thermocouples.

Table 2.2.4. Conditions for 5000-hr Corrosion Test Under Irradiation

Composition of fuel	Li^7F-BeF_2-$U^{235}F_4$ (62-37-1 mole %)
Melting point of fuel	842°F
Composition of INOR-8	Mo, 17%; Cr, 8%; Fe, 5%; Mn, 0.5%; C, 0.06%; bal Ni
Operating temperature	1250°F
Temperature control	Air-cooled
Weight of fuel per capsule	0.400 g
Power density (initial)	1.17 kw/cc
Thermal flux	$1\text{–}2 \times 10^{14}$ neutrons·cm^{-2}·sec^{-1}
Total hours in reactor	5508
Total hours above 842°F	3392
Total hours below 842°F	1883
Total hours not operating (shutdowns, etc.)	233
Integrated thermal flux	2×10^{21} nvt
Estimated uranium burnup	75%

2.3 FUEL PROCESSING

Emphasis is being placed on modification of the hydrofluorination–volatilization process for application to MSR salts containing ThF_4. The process as originally developed was satisfactory for the recovery of uranium from core and blanket salts in a two-region reactor and for the recycle of Li^7F and BeF_2 used in the core fuel.[1] There was no provision in this process, however, for the handling of thorium, which is particularly desirable in core salt, where frequent processing is necessary. The hydrofluorination–volatilization process has as an attractive feature the fact that the processed material remains in the fluoride form and thus requires little further treatment before re-use in the reactor. Retention of this feature is one objective of the work.

The use of hot aqueous NH_4F solution appears definitely promising for processing ThF_4-bearing fuels, and further work in this direction seems appropriate. The possibility of using ClF_3-HF as a solvent for the simultaneous solution of UF_4 and LiF no longer appears attractive because an appreciable concentration of ClF_3 represses the LiF solubility and because the solubilities of UF_4 and ThF_4 are unsatisfactory. The NO_2-HF system appears attractive for the simultaneous dissolution of LiF, BeF_2, and UF_4, but it does not show sufficient ThF_4 solubility.

Thorium Fluoride Solubility in Aqueous NH_4F Solutions

An exploratory test indicated that ThF_4 was soluble to about 5 wt % in 50 wt % aqueous NH_4F solution at the boiling point, which is high enough to be of interest for processing. Typical fuel salts contain about 60 wt % ThF_4. Experimental data indicated increasing ThF_4 solubility with increasing temperature and increasing NH_4F concentration, although some difficulties were encountered in sampling solutions at or near the boiling point. The ThF_4 solubility in 50% solution at 105°C was 49 mg/ml in a sample pipetted from a solution in which the solids had been allowed to settle, and was 43 mg/ml in a sample filtered through sintered nickel. The solubility dropped rapidly with decreasing temperature, to about 12 mg/ml at 60°C and 4.9 mg/ml at 25°C. In 43% NH_4F solution at 25°C the solubility was only

[1] H. G. MacPherson, Molten Salt Reactor Program Status Report, ORNL-2634 (Nov. 12, 1958).

0.4 mg/ml. The solid formed when these NH_4F solutions of ThF_4 were cooled or diluted was not ThF_4, but rather a compound (or compounds) involving NH_4F and ThF_4. The compositions of solids formed under various conditions are being determined.

The investigation is being extended to measurements of the solubilities of the other fuel components – LiF, BeF_2, UF_4, and rare earths – both individually and collectively. The effect of other components on the ThF_4 solubility has not been measured.

Fuel-Component Solubility in ClF_3-HF

Mixed ClF_3-HF solvent appears unsatisfactory for a one-step process to dissolve both uranium and LiF. Further experiments confirmed the observations reported previously[2] that ClF_3 in HF causes a drastic reduction in the LiF and BeF_2 solubilities with MSR fuel salt (LiF-BeF_2-ThF_4-UF_4, 62-36.5-1-0.5 mole %). The presence of significant amounts of ClF_3 in HF decreased the solubility of LiF from ~100 to ~20 g/kg, and of BeF_2 from 30–40 to < 5 g/kg. Uranium solubilities were generally about 0.25 g/kg; although significant, they are too low to dissolve all the uranium associated with the dissolved LiF and BeF_2. Rare-earth and thorium fluorides are very insoluble in these solutions; rare-earth solubilities were in the range 0.0001 to 0.0005 mole %, based on dissolved salt.

The U(IV), which has a low solubility, is probably not converted under these conditions to the highly soluble U(VI). Operation of the ClF_3-HF system at a higher temperature and pressure to obtain conversion appears impractical. Hence no further work in this direction is planned.

Fuel-Component Solubility in NO_2-HF

Scouting tests of the solubility of fuel salt (LiF-BeF_2-ThF_4-UF_4, 62-36.5-1-0.5 mole %, plus 0.05 mole % rare-earth fluorides and trace fission products) in NO_2-HF solutions were completed. The results (Table 2.3.1) show that LiF and BeF_2 have reasonably good solubility if the NO_2 content is not much higher than 5 mole % (above which LiF solubility drops) or much lower than probably 2 mole % (below which BeF_2 solubility drops). Uranium solubilities were generally about 1 g/liter, with some indication

[2]MSR Quar. Prog. Rep. July 31, 1959, ORNL-2799, p 96.

Table 2.3.1. Solubilities of Fuel Components and Fission Products in NO_2-HF Solutions

NO_2 (mole %)	Solubility					
	Major Components (g/kg)				Rare Earths (mole %)	
	LiF	BeF_2	U	Th	Based on Ce	Based on Pm
2.7	35	62	1.0	0.06	0.0013	0.0025
5.0	48	49	0.9	0.15	0.0006	0.001
10.0	19	36	1.4	0.04	0.001	0.0003

that values would be higher at NO_2 concentrations above 10 mole %; uranium solubilities are presumably high in the absence of LiF and BeF_2. Thorium solubilities were generally low, and rare-earth solubilities were mostly about 0.001 to 0.002 mole %, based on dissolved salt (the most reliable value, from an experiment discussed below, was 50-fold less than this).

With 2.7 mole % NO_2 (Table 2.3.1) the BeF_2 solubility was unexpectedly high, corresponding almost exactly with the NO_2 content on a mole basis. The LiF solubility was only about half as high as expected. The uranium solubilities account for about one-third of the uranium associated with the dissolved salt except with 10 mole % NO_2, where it accounts for all of it. With 5 mole % NO_2 the total salt solubility is a little over 100 g/liter, which is a reasonable value for processing.

In another experiment with approximately 2 mole % NO_2 in HF, the solution was decanted from the undissolved excess salt and both were analyzed separately. The LiF, BeF_2, uranium, and thorium solubilities were 33, 52, 0.5, and 0.04 g/kg, respectively, in reasonable agreement with the values reported above. The NO_2-HF solution dissolved 56% of the LiF, 79% of the BeF_2, 5% of the uranium, and 62% of the cesium activity, but only 0.086% of the cerium and 0.059% of the promethium. The much larger samples permitted more accurate determinations of the rare-earth activities than in the experiments reported in Table 2.3.1. The total rare-earth solubilities were 0.000042 mole % calculated from the cerium determination and 0.000029 mole % calculated from the promethium determinations, based on dissolved LiF and BeF_2.

The above results were obtained at room temperature. As NO_2 was added to HF, the boiling point rose rapidly to about 56°C at about 25 mole % NO_2 and then dropped to the boiling point of NO_2 (21°C) with about 60 mole % NO_2, at which point a second phase appeared. The second phase appeared to be nearly pure NO_2. Salt solubilities would probably be significantly higher at the boiling points, since salt solubilities in other HF systems have been observed to increase with temperature.

ORNL-2890
Reactors — Power
TID-4500 (15th ed.)

INTERNAL DISTRIBUTION

1. R. G. Affel
2. L. G. Alexander
3. E. S. Bettis
4. D. S. Billington
5. F. F. Blankenship
6. E. P. Blizard
7. A. L. Boch
8. C. J. Borkowski
9. W. F. Boudreau
10. G. E. Boyd
11. M. A. Bredig
12. E. J. Breeding
13. R. B. Briggs
14. W. E. Browning
15. D. O. Campbell
16. W. H. Carr
17. G. I. Cathers
18. C. E. Center (K-25)
19. R. A. Charpie
20. J. H. Coobs
21. F. L. Culler
22. J. H. DeVan
23. D. A. Douglas
24. L. B. Emlet (K-25)
25. W. K. Ergen
26. J. Y. Estabrook
27. D. E. Ferguson
28. A. P. Fraas
29. E. A. Franco-Ferreira
30. J. H. Frye, Jr.
31. W. R. Gall
32. A. T. Gresky
33. J. L. Gregg
34-36. W. R. Grimes
37. E. Guth
38. C. S. Harrill
39. M. R. Hill
40. E. E. Hoffman
41. H. W. Hoffman
42. A. Hollaender
43. A. S. Householder
44. W. H. Jordan
45. G. W. Keilholtz
46. C. P. Keim
47. M. T. Kelley
48. F. Kertesz
49. B. W. Kinyon
50. M. E. Lackey
51. J. A. Lane
52. R. S. Livingston
53. H. G. MacPherson
54. W. D. Manly
55. E. R. Mann
56. L. A. Mann
57. W. B. McDonald
58. H. F. McDuffie
59. J. R. McNally
60. H. J. Metz
61. R. P. Milford
62. E. C. Miller
63. J. W. Miller
64. K. Z. Morgan
65. J. P. Murray (Y-12)
66. M. L. Nelson
67. G. J. Nessle
68. W. R. Osborn
69. P. Patriarca
70. A. M. Perry
71. D. Phillips
72. W. D. Reel
73. P. M. Reyling
74. J. T. Roberts
75. M. T. Robinson
76. H. W. Savage
77. J. L. Scott
78. H. E. Seagren
79. E. D. Shipley
80. M. J. Skinner
81. G. M. Slaughter
82. A. H. Snell
83. E. Storto
84. C. D. Susano
85. J. A. Swartout
86. A. Taboada
87. E. H. Taylor
88. R. E. Thoma
89. D. B. Trauger
90. F. C. VonderLage

91. G. M. Watson
92. A. M. Weinberg
93. M. E. Whatley
94. J. C. White
95. G. D. Whitman
96. G. C. Williams
97. C. E. Winters
98. J. Zasler
99-102. ORNL - Y-12 Technical Library, Document Reference Section
103-142. Laboratory Records Department
143. Laboratory Records, ORNL R.C.
144-145. Central Research Library

EXTERNAL DISTRIBUTION

146. D. H. Groelsema, AEC, Washington
147. Division of Research and Development, AEC, ORO
148-742. Given distribution as shown in TID-4500 (15th ed.) under Reactors-Power category (75 copies - OTS)